The Canadian Mineralogist
Vol. 37, pp. 177-198 (1999)

CALCITE – AMPHIBOLE – CLINOPYROXENE ROCK FROM THE AFRIKANDA COMPLEX, KOLA PENINSULA, RUSSIA: MINERALOGY AND A POSSIBLE LINK TO CARBONATITES. I. OXIDE MINERALS[1]

ANTON R. CHAKHMOURADIAN

Department of Geology, Lakehead University, 955 Oliver Road, Thunder Bay, Ontario P7B 5E1

ANATOLY N. ZAITSEV

Department of Mineralogy, St. Petersburg State University, 7/9 University Emb., St. Petersburg, 199034, Russia

Abstract

A calcite – amphibole – clinopyroxene rock (CAPR) occurs as branching veins and segregations in ultramafic alkaline lithologies of the Afrikanda complex, Kola Peninsula, in Russia. The rock is composed predominantly of diopside, magnesiohastingsite, calcite, titanite, chlorite and oxide phases. In the present study, a complete characterization of morphology, interrelations, and compositional variation of the oxide minerals is given, and eleven phases are described at Afrikanda for the first time. Three parageneses are distinguished among the oxide minerals, based on their geochemical features and relative position in the crystallization history. These are (in order of formation): primitive (early magnetite, lamellar ilmenite, primary perovskite, baddeleyite, calzirtite, zirconolite), evolved (secondary perovskite, loparite, lueshite, betafite, late magnetite, discrete ilmenite, thorutite, thorianite) and replacement (rutile, hematite, fersmite, pyrochlore, an unidentified *REE*–Ti oxide) associations. The primitive and evolved associations formed in the temperature range 500–550°C at $f(O_2)$ approximately 10^{-20} – 10^{-22} bar, and $a(SiO_2)$ generally below $10^{-1.2}$. The replacement assemblage crystallized immediately prior to the precipitation of calcite under increasing $a(SiO_2)$ and $f(O_2)$ (? decreasing temperature). This assemblage is closely associated with late silicate minerals, including titanite, chlorite and Zr-bearing silicates. The complex mineralogy of CAPR cannot be explained in terms of simple differentiation of a parental silicocarbonatitic melt. The textural and mineralogical features indicate that the evolution of CAPR involved substantial interaction between a CO_2-rich liquid (? fluid) and the ultramafic wallrocks.

Keywords: magnetite, perovskite, ilmenite, Zr oxides, thorutite, pyrochlore, carbonatite, clinopyroxenite, Afrikanda, Kola Peninsula, Russia.

Sommaire

On trouve, dans le complexe ultramafique alcalin de Afrikanda, dans la péninsule de Kola, en Russie, une roche à calcite – amphibole – clinopyroxène sous forme de veines ramifiées et de ségrégations. Cette roche contient surtout diopside, magnésiohastingsite, calcite, titanite, chlorite et des oxydes. Nous présentons ici une caractérisation complète de la morphologie, des inter-relations, et des variations en composition des oxydes; onze minéraux sont ici décrits dans de telles roches à Afrikanda pour la première fois. Nous distinguons trois associations paragénétiques, selon les aspects géochimiques et la position relative dans la séquence de cristallisation. Il s'agit (dans l'ordre de leur formation) des associations primitive (magnétite, ilménite lamellaire, pérovskite, baddeleyite, calzirtite, zirconolite), évoluée (pérovskite secondaire, loparite, lueshite, bétafite, magnétite tardive, ilménite individualisée, thorutite, thorianite) et de remplacement (rutile, hématite, fersmite, pyrochlore, oxyde à terres rares et titane non identifié). Les associations paragénétiques primitive et évoluée se seraient formées dans l'intervalle 500–550°C à une fugacité d'oxygène $f(O_2)$ d'environ 10^{-20}–10^{-22} bar, et une activité de silice $a(SiO_2)$ généralement inférieure à $10^{-1.2}$. L'assemblage dû au remplacement a cristallisé immédiatement avant la précipitation de la calcite dans un milieu augmentant en $a(SiO_2)$ et $f(O_2)$ (et peut-être avec diminution de la température). Cet assemblage est intimement associé aux minéraux silicatés tardifs, par exemple titanite, chlorite et silicates zirconifères. La minéralogie compliquée de ces roches à calcite – amphibole – pyroxène ne pourrait pas découler d'un simple schéma de différenciation d'un magma parental silicocarbonaté. D'après les attributs texturaux et minéralogiques, l'évolution de telles roches aurait impliqué une interaction importante entre un liquide ou fluide à base de CO_2 et l'encaissant ultramafique.

(Traduit par la Rédaction)

Mots-clés: magnétite, pérovskite, ilménite, oxydes de Zr, thorutite, pyrochlore, carbonatite, clinopyroxénite, Afrikanda, péninsule de Kola, Russia.

E-mail addresses: achakhmo@gale.lakeheadu.ca, zaitsev@mineral.geol.pu.ru

[1] This work is dedicated to the memory of our close friend, petrologist Max Poritskiy (1968–1995), who is sorely missed.

Introduction

The Paleozoic Kola Alkaline Province covers an area of approximately 100,000 km^2, and is one of the largest carbonatite provinces in the world. It includes at least 13 alkaline ultramafic complexes that were emplaced during the Middle to Late Devonian re-activation of the ancient rift zones developed within the Fenno-Scandinavian Shield (Kukharenko *et al.* 1965, Kramm *et al.* 1993, Orlova 1993). The complexes comprise an extended series of ultramafic, alkaline and carbonatitic rocks. These may represent products of differentiation of a single parental alkaline ultramafic magma (Kukharenko *et al.* 1965, 1971, Bulakh & Ivanikov 1984, 1996) or, alternatively, derivatives from several sources in the mantle (Zaitsev & Bell 1995). Formation of some complexes, *e.g.,* Turiy Mys (Cape), involved several pulses of magmatic activity over a continuous period of time (Bulakh & Ivanikov 1984). The geology, petrography and geochemistry of most alkaline ultramafic intrusions in the Kola Province were described in detail by Kukharenko *et al.* (1965, 1971).

Despite more than seventy years of research and exploration, many aspects of the geology of the Kola carbonatite complexes still generate impassioned scientific discussion. One of these aspects is the genesis and evolution of Ca-rich silicate rocks that are commonly associated with carbonatites. These include a broad variety of texturally and mineralogically diverse melilite-, monticellite-, garnet-, clinopyroxene- and amphibole-bearing rocks referred to as "autometasomatic" in the Russian geological literature. One example is a calcite – amphibole – clinopyroxene rock occurring at the Afrikanda complex, also known as pegmatitic pyroxenite, amphibole pyroxenite or vibetoite (Kukharenko *et al.* 1965). Although the first description of this unusual calcite-rich rock was given sixty years ago (Kupletskii 1938), its relative position in the evolution of the Afrikanda complex remains incompletely understood. The rock is composed predominantly of calcite, amphibole and clinopyroxene, with lesser amounts of titanite, magnetite and perovskite, and occurs as branching veins within the ultramafic members of the suite. On the basis of the petrographic classification of Streckeisen (1978), this rock may be regarded as a series from calcite-bearing clinopyroxenite through calcite clinopyroxenite to calcite-carbonatite. In this work, we prefer to use the descriptive term "calcite – amphibole – clinopyroxene rock" (hereafter CAPR). It is based solely on the modal mineralogy and has no genetic connotation, *i.e.* not implying an intrusive mode of emplacement or igneous nature of the calcite.

Most investigators agree that CAPR is genetically related to the ultramafic lithologies comprising the bulk of the Afrikanda intrusion. Kupletskii (1938) interpreted CAPR as an igneous rock, containing primary calcite. Kukharenko *et al.* (1965) suggested that CAPR is a product of deuteric ("autometasomatic") alteration of clinopyroxenite. Alternatively, the high modal content of calcite (locally up to 90%), as well as the presence of pyrochlore, zirconolite, baddeleyite and some other Nb- and Zr-bearing minerals, may indicate a close affinity between CAPR and carbonatites. There has been no systematic mineralogical study of this enigmatic rock; the only description of the major and some accessory phases in CAPR was published more than three decades ago (Kukharenko *et al.* 1965). With a few exceptions [perovskite: Chakhmouradian & Mitchell 1997, 1998a; calcio-ancylite-(Ce): Pekov *et al.* 1997], virtually no data on the compositional variation of major and accessory minerals from CAPR are available in the literature. The present work is the first in a series of studies based on the mineralogical approach to the genesis and evolution of calcite – amphibole – clinopyroxene rock at Afrikanda. This approach has been chosen because most of the major and accessory constituents of this rock (clinopyroxene, garnet, amphibole, perovskite, ilmenite, among others) have a high capacity for cationic substitutions, and thus are important indicators of geochemical evolution. In the present study, we describe the occurrence and compositional variation of oxide phases from CAPR. The silicate and oxysalt minerals will be characterized in subsequent publications. The samples used in this work were collected by the authors mostly from outcrops over the interval 1992–1997.

Geological Setting

The Afrikanda complex is emplaced into a Precambrian metamorphic sequence comprising primarily biotite–plagioclase gneiss of the Belomorskii suite. The nearly circular intrusive body covers an area of approximately 11.5 km^2 at the current level of erosion, and shows a concentric internal structure. The latter results from successive emplacement of major intrusive phases during the formation of the complex. The oldest igneous rocks exposed at Afrikanda are olivinites. (Here, we use the term "olivinite" instead of dunite to emphasize that titaniferous magnetite and perovskite, not chromite, are major opaque minerals in these rocks). The olivinites are found as xenoliths in the younger units, predominantly in clinopyroxenites. The xenoliths vary from small angular fragments to large (tens of cubic meters) elliptical or round blocks. The xenoliths are composed mostly of fine-grained olivinite with subordinate lenses and veinlets of coarse-grained and porphyritic melilite-bearing varieties. The second intrusive phase led to texturally and modally diverse clinopyroxenites. From the center of the intrusion outward, coarse-grained clinopyroxenite grades to a fine-grained, and then to a nepheline-bearing variety. Locally within the rim of the intrusion, nepheline is a major rock-forming mineral, and the nepheline-bearing clinopyroxenite grades into melteigite. Olivine- and feldspar-bearing clinopyroxenites are hybrid rocks interpreted to originate by contamination of "normal" clinopyroxenite with mate-

rial assimilated from the olivinites and fenitized gneiss, respectively (Kukharenko *et al.* 1965).

Alkaline rocks of the melteigite–urtite series represent the third intrusive phase at Afrikanda; these are less common than the ultramafic rocks. The foidolites are developed as dikes and pegmatite veins intruding the ultramafic units. Contacts between the alkaline and ultramafic rocks vary from sharp, intrusive to diffuse, resulting from fine injections of an alkaline melt into the host rock, and replacement of mafic minerals by nepheline (Bagdasarov 1959). At the contact with foidolites, ultramafic rocks are commonly enriched in phlogopite, magnetite, amphibole and apatite.

CAPR is developed primarily in the central part of the Afrikanda intrusion. It occurs as branching veinlets and irregular segregations in the ultramafic suite. The bodies of CAPR vary from a few centimeters to 1.8–2.0 m in thickness. The rock is massive and very coarse-grained to pegmatitic. In CAPR, most major and accessory minerals occur as euhedral crystals ranging from a few millimeters to several centimeters in size. Contacts between CAPR and the ultramafic wallrocks (primarily clinopyroxenite) are invariably diffuse; the latter are typically enriched in amphibole and calcite at the contact. The contact zones of CAPR consist mostly of silicates (clinopyroxene, amphibole, garnet) and oxides (magnetite plus perovskite). At selvages, the rock is patchy in appearance, with grayish green, black, white and honey-yellow colors produced by randomly distributed crystals of clinopyroxene, amphibole, magnetite, perovskite, calcite and titanite. The central parts of the bodies are composed predominantly of calcite with minor ilmenite, chlorite and zircon. The modal percentages of major constituents, as well as the distribution of minor accessory minerals in CAPR, may change significantly over a short distance. On an overall scale, however, clinopyroxene (diopside), amphibole (mostly magnesiohastingsite), calcite, magnetite and perovskite remain the major rock-forming phases.

TABLE 1. REPRESENTATIVE COMPOSITIONS OF MAGNETITE FROM CALCITE-AMPHIBOLE-DIOPSIDE ROCK

Wt.%	1	2	3	4	5	6
MgO	1.64	0.47	0.35	0.34	0.25	0.16
MnO	1.07	0.32	0.45	0.58	0.20	0.42
FeO*	26.82	23.57	22.98	22.87	25.02	26.23
Fe_2O_3*	63.88	76.26	74.72	75.70	70.44	68.94
Al_2O_3	0.97	0.31	0.13	0.24	0.07	n.d
TiO_2	6.36	0.84	0.80	0.53	2.82	3.95
Total	100.74	101.77	99.43	100.26	98.80	99.70
Structural formulae calculated on the basis of 4 atoms of oxygen:						
Mg	0.092	0.027	0.020	0.020	0.014	0.009
Mn	0.034	0.010	0.015	0.019	0.007	0.014
Fe^{2+}	1.054	0.987	0.988	0.977	1.062	1.092
Fe^{3+}	1.597	1.938	1.947	1.958	1.831	1.770
Al	0.043	0.014	0.006	0.011	0.003	-
Ti	0.180	0.024	0.023	0.015	0.083	0.115

Compositions: 1 - 4 early magnetite, 1 & 2 core and rim of large (3.5 cm) euhedral crystal with ilmenite lamellae, 3 & 4 core and rim of small (2.2 mm) euhedral crystal with ilmenite lamellae, 5 & 6 late lamella-free magnetite (euhedral crystals 40-50 μm across). * FeO/Fe_2O_3 ratio is calculated from stoichiometry.

All mineral compositions in this study were determined by X-ray energy-dispersion spectrometry using a Hitachi 570 scanning electron microscope equipped with a LINK ISIS analytical system. Operating conditions: 20 kV, 0.86 nA; standards: ilmenite (Fe, Ti), perovskite (Ca), loparite (Na, *REE*, Nb), wollastonite (Si), manganiferous olivine (Mn), corundum (Al), periclase (Mg), synthetic $SrTiO_3$ (Sr), metallic Zr, Hf, Ta, Th, U. Compositions of zirconolite were also determined by wavelength-dispersion spectrometry (see Table 5 for details).

Occurrence and Chemistry of Oxide Minerals

Magnetite is a common mineral in CAPR. Locally within the silicate-rich zones in CAPR, magnetite and perovskite comprise up to 50 vol.% of the rock. In this work, we distinguish two generations of the mineral. The early generation consists of large (up to 5 cm) octahedral crystals associated with clinopyroxene, amphibole and perovskite. These are common in the silicate-rich zones near the contact and are not found in the calcite-rich zones near the core. The late generation occurs as minute (tens of μm) euhedral crystals enclosed in calcite and discrete ilmenite. In contrast to the late generation, the early magnetite contains ilmenite lamellae that are predominantly concentrated in the marginal zones of the crystals.

Large (> 1 cm) crystals of early magnetite are compositionally inhomogeneous. The core of the crystals is enriched in Ti, Mg, Mn and, to a lesser extent, Al relative to the rim (Table 1, anals. 1–2). Smaller crystals densely populated with the lamellae of ilmenite normally do not show any compositional zonation (Table 1, anals. 3–4). A core-to-rim pattern of zonation, with decreasing Mg and decreasing or constant Ti and Mn, has been previously described for magnetite from various carbonatite facies in the East African complexes (Prins 1972), Sarfartôq, Greenland (Secher & Larsen 1980) and Jacupiranga, Brazil (Gaspar & Wyllie 1983a). In our case, the depletion in Ti, Mn and Mg toward the rim resulted from the oxidation of primary titaniferous magnetite and preferential accumulation of these elements in the lamellar ilmenite. The data obtained in this study and previously published results of bulk analyses

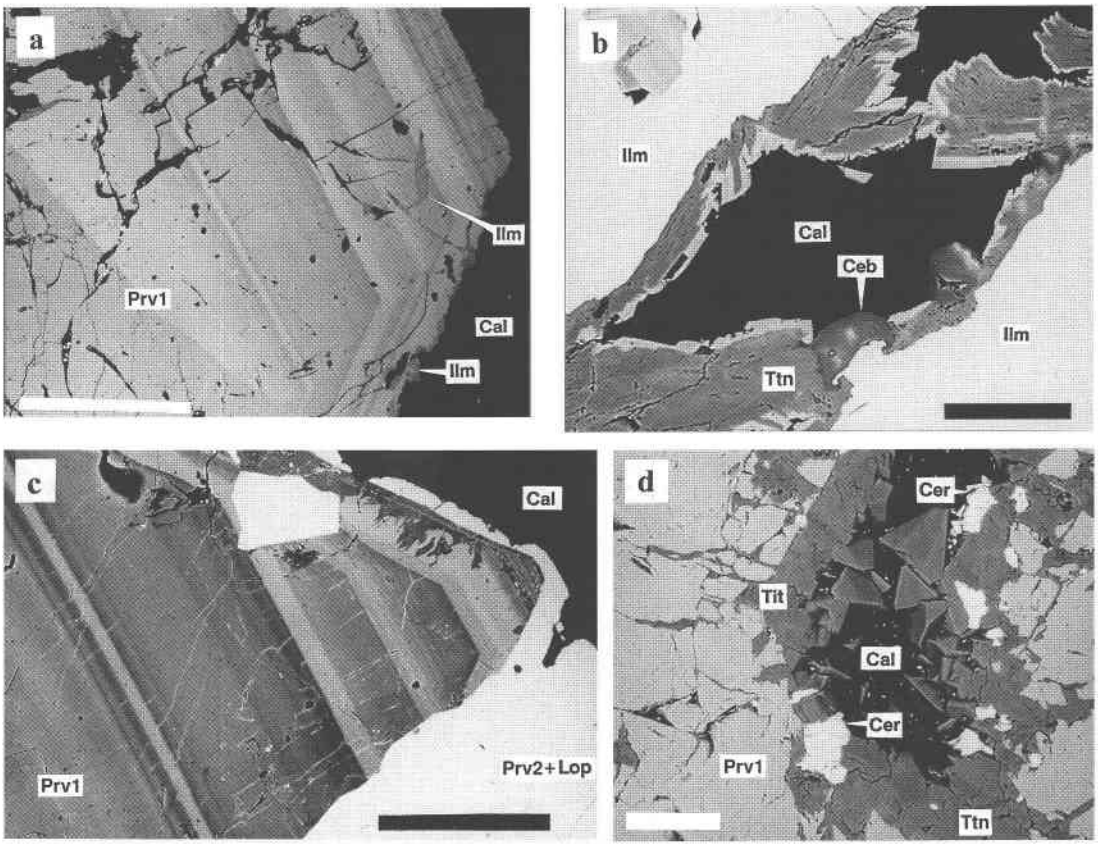

FIG. 1. Morphology of perovskite and ilmenite from calcite – amphibole – clinopyroxene rock, Afrikanda complex. Back-scattered electron (BSE) images. (a) Discrete ilmenite (Ilm) filling fractures in primary perovskite (Prv1); scale bar is 750 μm. (b) Encrustation of titanite (Ttn) and cebollite (Ceb) at the contact between discrete ilmenite (Ilm) and calcite (Cal); scale bar is 120 μm. (c) Secondary Na–*REE*-rich perovskite and loparite (Prv2 + Lop) rimming primary perovskite (Prv1). Note the change in morphology of primary perovskite from the pseudohexahedral core to the pseudocubo-octahedral outer zones; contrast between secondary perovskite and loparite could not be resolved without extinguishing the image of primary perovskite; scale bar is 600 μm. (d) Titanite (Ttn) lining a cavity and filling fractures in primary perovskite (Prv1); the cavity also hosts cerite-(Ce) (Cer) and calcite (Cal); scale bar is 90 μm.

(Kukharenko *et al.* 1965, Table 55) suggest that the primary magnetite contained up to 8.8 wt.% TiO_2, 1.6% MgO and 1.2% MnO. Compared to the early magnetite from CAPR, magnetite from carbonatites is normally poorer in Ti, whereas magnetite from ultramafic rocks, including those exposed at Afrikanda, has comparable Ti, but is typically richer in Mg and Al (Kukharenko *et al.* 1965, Prins 1972, Bagdasarov 1980, Secher & Larsen 1980, Gaspar & Wyllie 1983a, Egorov 1991, Knudsen 1991).

The late generation of magnetite from CAPR is poor in Mg, Mn and Al. In terms of Mg, Mn and Al contents, this mineral is similar to the Ti-depleted rim on grains of the early magnetite, but contains higher Ti. Compared to the cores of the early magnetite, the late generation is significantly poorer in Mg, Mn, Al and Ti (Table 1, anal. 5, 6), and falls into the range of "typical" magnetite from carbonatites. The absence of ilmenite inclusions in the late magnetite, and the small size of its crystals, suggest rapid crystallization, probably combined with very low $f(O_2)$ in the system.

Ilmenite occurs as lamellae in the early magnetite and discrete platy crystals up to 2.5 cm across. Two morphological types of lamellar ilmenite are observed in back-scattered electron images (BSE). There are long thin lamellae oriented parallel to {111} of the magnetite host, and coarse irregular laths distributed at random. These two types of ilmenite can be classified as the trellis- and sandwich-type lamellae, respectively (Haggerty 1991). The sandwich-type laths are typically

TABLE 2. REPRESENTATIVE COMPOSITIONS OF ILMENITE, TITANIFEROUS HEMATITE AND THORUTITE FROM CALCITE-AMPHIBOLE-DIOPSIDE ROCK

Wt.%	1*	2*	3*	4*	5	6	7	8*	9*	10	11	12*	13**
MgO	4.70	0.15	0.59	4.97	6.52	6.05	1.16	1.38	1.25	1.63	1.43	0.02	n.d
MnO	16.19	10.41	2.82	4.45	3.60	5.07	2.08	3.44	2.20	2.32	2.22	0.76	n.d
FeO	23.60	36.63	43.71	33.69	33.22	33.06	42.87	42.61	41.86	42.66	40.82	5.87	n.d
Fe_2O_3	1.51	n.d	n.d	4.56	3.37	1.89	n.d	0.24	3.52	n.d	n.d	83.17	1.36
ThO_2	n.a	n.a	n.a	n.a	n.a	n.a	n.a	n.a	n.a	n.a	n.a	n.a	61.45
TiO_2	53.91	52.83	52.96	52.80	54.20	54.66	53.26	54.03	51.39	54.32	52.58	9.81	36.60
Nb_2O_5	n.d	n.d	n.d	n.d	0.05	n.d	0.58	n.d	0.47	0.17	1.41	n.d	n.d
Total	99.91	100.02	100.08	100.47	100.96	100.73	99.95	101.70	100.69	101.10	98.46	99.63	99.41
Structural formulae calculated on the basis of:													
						ΣO = 3							ΣO = 6
Mg	0.171	0.006	0.022	0.180	0.232	0.216	0.043	0.050	0.046	0.060	0.054	0.001	-
Mn	0.334	0.222	0.060	0.091	0.073	0.103	0.044	0.072	0.046	0.048	0.047	0.017	-
Fe^{2+}	0.483	0.771	0.918	0.692	0.668	0.666	0.896	0.876	0.881	0.878	0.862	0.177	-
Fe^{3+}	0.026	-	-	0.074	0.054	0.031	-	0.004	0.058	-	-	1.609	0.072
Th	-	-	-	-	-	-	-	-	-	-	-	-	0.992
Ti	0.987	1.000	1.000	0.963	0.972	0.985	1.000	0.998	0.963	1.005	0.998	0.195	1.952
Nb	-	-	-	-	0.001	-	0.006	-	0.005	0.002	0.016	-	-

Compositions: 1 - 3 sandwich-type ilmenite lamellae in magnetite, 4 - 6 trellis-type ilmenite lamellae in magnetite, 7 ilmenite crystal in a fracture within primary perovskite, 8 - 11 discrete ilmenite crystals, 12 rim of titaniferous hematite on discrete ilmenite, 13 thorutite "lamella" in discrete ilmenite. n.a = not analyzed, n.d = not detected. * FeO/Fe_2O_3 ratio is calculated from stoichiometry; ** Total Fe is given as Fe_2O_3.

less than 300 μm in length and up to 100 μm in thickness. The trellis-type lamellae may be up to several millimeters in length, but do not exceed 15 μm in thickness. Both types of lamellae are found predominantly at the margin of magnetite crystals, suggesting that the lamellae were produced by oxidation of initially homogeneous titaniferous magnetite. The observed textural features correspond to the C3 stage of the "oxyexsolution" process (*sensu* Haggerty 1991). A few sandwich-type laths of ilmenite contain rare thin needles of rutile, indicating further oxidation toward the C4 stage. Some magnetite crystals are fractured along the lamellae. The fractures are filled with titanite, chlorite or calcite, and contain minute (up to 20–25 μm) euhedral crystals of baddeleyite, calzirtite, barite, sphalerite and pyrrhotite.

The discrete crystals and sheaf-like intergrowths of ilmenite are set in the calcite matrix or fill fractures within perovskite, garnet and some other minerals (Fig. 1a). Individual crystals rarely exhibit pinacoid and poorly developed rhombohedral faces. At the contact with calcite, the discrete ilmenite typically shows a reaction rim of titanite (Fig. 1b). This ilmenite was formed after the early magnetite, perovskite-group minerals and most silicates, but prior to calcite and chlorite.

The lamellar ilmenite demonstrates significant compositional variation with respect to Mg, Mn, Fe, Ti, but contains no detectable Nb (Table 2). The lamellae are relatively poor in Fe^{3+} (<7.3 mol.% Fe_2O_3); hence, the diagram $FeTiO_3$ – $MgTiO_3$ – $MnTiO_3$ is used to illustrate the compositional variation of ilmenite. The sandwich-type lamellae predate those of the trellis type, and show a wide range from Mg- and Mn-enriched compositions to almost pure $FeTiO_3$ (Table 2, anals. 1–3; Fig. 2). Mn- and Mg-rich ilmenite has been previously described from the carbonatite ("unit 4") of the Jacupiranga complex, Brazil (Gaspar & Wyllie 1983b). In contrast to Afrikanda, the most Mn-rich ilmenite at Jacupiranga occurs as discrete crystals, not inclusions in magnetite, and is significantly enriched in Nb (1.1–3.4 wt.% Nb_2O_5: Gaspar & Wyllie 1983b). The trellis-type lamellae are relatively uniform in composition (Table 2, anals. 4–6) and plot near the field of typical ilmenite from carbonatites (Fig. 2 and references therein).

Ilmenite occurring as discrete crystals in the calcite matrix, and that found in fractures within perovskite and silicate minerals, are compositionally identical (Fig. 2), and most probably represent the same generation. This ilmenite is relatively poor in Mg, Mn and Fe^{3+} (Table 2, anals. 8–11). Some crystals show a weak intragranular variation in Nb (anals. 10–11), but no correlation in distribution of Nb within a crystal could be established. At the rim and along fractures, the discrete crystals of ilmenite are oxidized to titaniferous hematite (Table 2, anal. 12). Discrete ilmenite of similar composition occurs at many carbonatite localities, including Kovdor, Sebljavr, Vuorijarvi and Turiy Mys on the Kola Peninsula (Lapin 1979, Garanin *et al.* 1980, Kopylova *et al.* 1985, this work) and Sarfatoq in West Greenland (Secher & Larsen 1980). Compared to these, discrete ilmenite from Jacupiranga is enriched in Mg ("beforsite unit") or Mg, Mn and Nb ("unit 4") (Gaspar & Wyllie 1983b).

Thorutite is rare and found solely as "lamellar" inclusions in platy ilmenite. The laths of thorutite are a

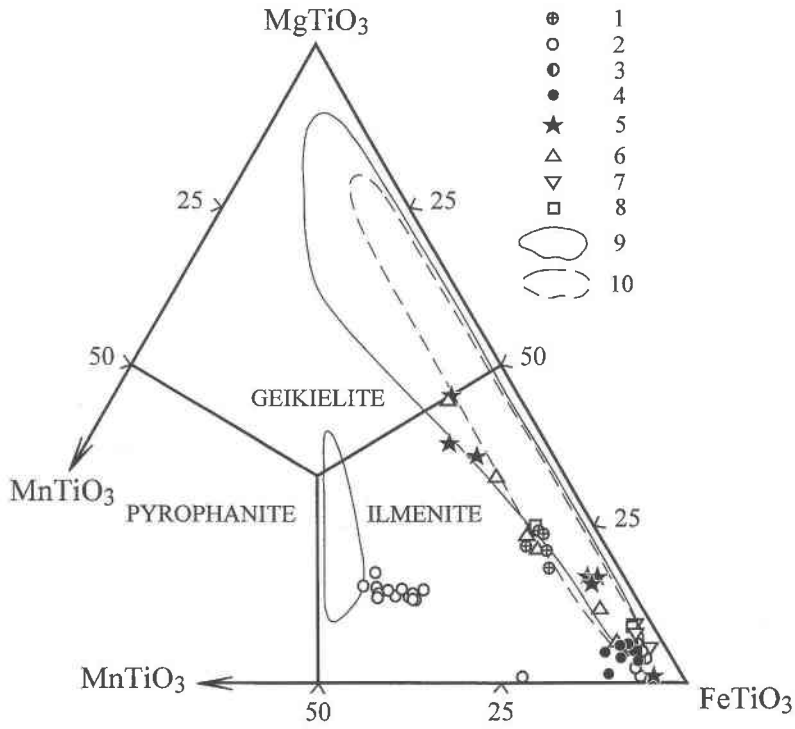

FIG. 2. Composition (mol.%) of ilmenite from calcite – amphibole – clinopyroxene rock and carbonatites: 1–4 Afrikanda: 1 trellis-type lamellae in early magnetite, 2 sandwich-type lamellae in early magnetite, 3 fracture fillings in primary perovskite and garnet, 4 discrete crystals in calcite groundmass; 5–10 carbonatites: Sebljavr, Kola (Garanin *et al.* 1980, Mitchell & Chakhmouradian 1998b), 6 Vuorijarvi, Kola (Garanin *et al.* 1980, this work), 7 Turiy Mys, Kola (Garanin *et al.* 1980), 8 Qaquarssuk, Greenland (Knudsen 1991), 9 Jacupiranga, Brazil (Mitchell 1978, Gaspar & Wyllie 1983b), 10 Kovdor, Kola (Kopylova *et al.* 1985, Krasnova & Balmasov 1987, Krasnova & Krezer 1995, Krasnova *et al.* 1991).

few tens of μm in length, and are oriented parallel to (0001) of the ilmenite host. It is noteworthy that one of the two known synthetic polymorphs of $ThTi_2O_6$ has a structure similar to that of ilmenite (Balić Žunić *et al.* 1984). In this polymorph, TiO_6 octahedra are arranged in a honeycomb-like fashion, and constitute layers parallel to (100). Dimensionally and geometrically, these layers of octahedra are analogous to the (0001) planes in the structure of ilmenite [*cf.* $c(ThTi_2O_6) = 5.192$ Å and $a(FeTiO_3) = 5.079$ Å]. Therefore, the orientation of thorutite "lamellae" may indicate their epitactic growth on the ilmenite substrate. The structure of naturally occurring thorutite has not been determined. The XRD powder pattern given by Gotman & Khapaev (1958) for the type material probably represents a mixture of phases, as it does not match those of synthetic Th titanates.

Compositionally, thorutite from Afrikanda is close to the ideal formula $ThTi_2O_6$ and contains only minor Fe (Table 2, anal. 13). On the basis of crystal chemistry, we assigned all Fe to Fe^{3+} substituting for Ti^{4+} in the TiO_6 octahedra:

$$Ti^{4+} + O^{2-} \rightarrow Fe^{3+} + (OH)^{1-}.$$

Thorutite is an extremely rare mineral and has not been previously described in alkaline ultramafic or carbonatitic rocks. The known occurences of thorutite include a syenite massif in Russia (Gotman & Khapaev 1958), and zirconolite-bearing placers at Walaweduwa, Sri Lanka (de Hoog & van Bergen 1997). In contrast to the Afrikanda thorutite, that from Russia and Sri Lanka shows minor substitutions of Ti by Nb, and Th by U (Gotman & Khapaev 1958, de Hoog & van Bergen 1997).

Perovskite-group minerals. The first description of perovskite from CAPR was made by Kukharenko & Bagdasarov (1961). Recently, Chakhmouradian &

TABLE 3. REPRESENTATIVE COMPOSITIONS OF PEROVSKITE-GROUP MINERALS FROM CALCITE-AMPHIBOLE-DIOPSIDE ROCK

Wt.%	1	2	3	4	5	6	7	8	9	10*
CaO	38.73	33.60	31.31	23.99	1.45	5.62	4.81	4.28	4.37	0.31
SrO	0.22	0.47	0.70	0.36	0.97	0.35	0.43	0.46	0.31	0.32
Na_2O	0.23	1.31	1.74	3.64	7.72	8.85	9.81	10.61	7.27	16.45
La_2O_3	0.34	0.94	1.33	2.49	11.17	6.18	5.43	5.29	3.63	n.d
Ce_2O_3	1.43	4.19	4.33	9.93	23.44	14.68	13.67	12.05	10.05	n.d
Pr_2O_3	n.d	0.91	0.65	1.36	1.78	1.23	1.43	1.11	1.25	n.d
Nd_2O_3	n.d	1.90	2.71	3.90	5.98	5.16	4.26	3.53	3.99	n.d
ThO_2	0.17	0.53	1.73	1.71	n.d	3.64	3.80	2.87	15.13	n.d
TiO_2	55.75	52.69	51.21	50.87	44.36	34.49	30.39	26.62	33.07	2.15
Fe_2O_3	0.91	1.23	1.11	0.80	0.03	0.46	0.39	0.59	0.36	1.24
Nb_2O_5	0.32	1.55	1.66	1.94	0.78	17.08	24.68	30.56	19.58	77.32
Ta_2O_5	0.42	0.22	0.27	0.40	1.65	0.99	0.98	1.51	0.55	2.01
Total	98.52	99.54	98.75	101.38	99.33	98.73	100.08	99.48	99.56	98.24
	Structural formulae calculated on the basis of 3 atoms of oxygen									
Ca	0.969	0.866	0.827	0.644	0.046	0.174	0.147	0.131	0.138	0.009
Sr	0.003	0.007	0.010	0.005	0.017	0.006	0.007	0.008	0.005	0.005
Na	0.011	0.061	0.083	0.177	0.442	0.496	0.544	0.589	0.416	0.887
La	0.003	0.008	0.012	0.023	0.122	0.066	0.057	0.056	0.039	-
Ce	0.012	0.037	0.039	0.091	0.253	0.155	0.143	0.126	0.108	-
Pr	-	0.008	0.006	0.012	0.019	0.013	0.015	0.012	0.013	-
Nd	-	0.016	0.024	0.035	0.063	0.053	0.044	0.036	0.042	-
Th	0.001	0.003	0.010	0.010	-	0.024	0.025	0.019	0.101	-
Ti	0.979	0.954	0.949	0.958	0.985	0.750	0.653	0.573	0.733	0.032
Fe	0.016	0.022	0.021	0.015	0.001	0.010	0.008	0.013	0.008	-
Nb	0.003	0.017	0.018	0.022	0.010	0.223	0.319	0.396	0.261	0.953
Ta	0.003	0.001	0.002	0.003	0.013	0.008	0.008	0.012	0.004	0.015

Compositions: 1 relict fine-grained perovskite, 2 & 3 primary perovskite, 4 secondary Na-*LREE*-rich perovskite, 5 loparite, 6 - 9 Nb-Th-rich loparite, 10 lueshite (inclusion in ilmenite).
* Structural formula calculated assuming 1.74 wt.% ilmenite in the analysis. n.d = not detected. Total Fe is given as Fe_2O_3.

Mitchell (1997, 1998a) have re-investigated perovskite-group minerals from some alkaline ultramafic complexes of the Kola Peninsula, including Afrikanda. These authors have established the major trends of compositional evolution of perovskite from the silicate and carbonatitic rocks. In CAPR, perovskite is found predominantly in an assemblage with early magnetite, clinopyroxene, amphibole, garnet and titanite. Perovskite occurs as three textural types:

(i) Fine-grained aggregates consist of anhedral to subhedral crystals less than 1 mm in size. The crystals are commonly corroded and replaced by honey-yellow titanite along the rim. Complete pseudomorphs of titanite after this perovskite are not uncommon. In thin section, this perovskite is grayish yellow in plane-polarized light, and shows anomalous bluish gray interference-colors. The crystals display complex, "patchy" zonation in back-scattered electron (BSE) images. The various zones are similar in composition and show only a slight variation in the light rare-earth elements (*LREE*). This perovskite is relatively poor in Na, *LREE*, Fe and Nb, and approaches the ideal formula $CaTiO_3$ (Table 3, anal. 1). Texturally and compositionally identical perovskite is found in the coarse-grained clinopyroxenite cut by CAPR veins (Chakhmouradian & Mitchell 1997, 1998a). Therefore, we interpret the fine-grained perovskite as xenocrysts derived from the ultramafic rocks.

(ii) Large euhedral crystals range in habit from pseudocubic to pseudo-octahedral. Rhombic pseudo-dodecahedron faces are much less common. In BSE, some large crystals show morphological evolution from a pseudocubic core to pseudocubo-octahedral external habit (Fig. 1c). This perovskite (termed primary perovskite hereafter) commonly encloses grains of xenocrystic perovskite and early magnetite. Faces of the perovskite crystals adjacent to amphibole show a dis-

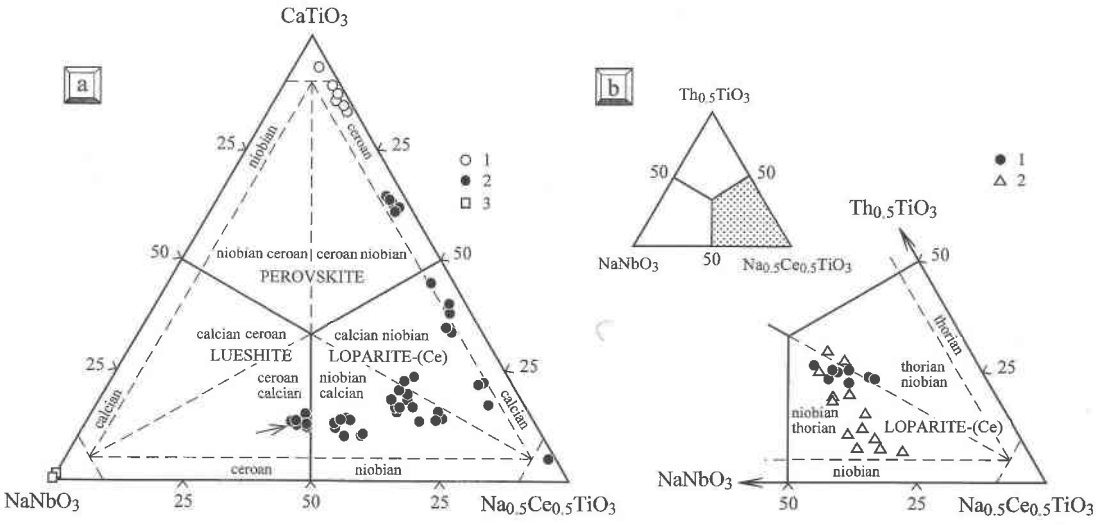

FIG. 3. Composition (mol.%) of perovskite-group minerals from calcite – amphibole – clinopyroxene rock. (a) Evolution of the perovskite composition: 1 primary perovskite, 2 secondary perovskite and loparite (mantles on primary perovskite), 3 lueshite (inclusions in discrete ilmenite); (b) Th-rich loparite: 1 Afrikanda, 2 Khibina (Mitchell & Chakhmouradian 1998a).

tinct induced striation (*sensu* Grigor'ev 1965, p. 187). Fractures in the crystals are filled with ilmenite, titanite, chlorite and calcite (Figs. 1a, d). Some of the fractures also host pyrochlore-group minerals, cerite-(Ce), ancylite-(Ce) and thorianite. The primary perovskite was formed nearly simultaneously with amphibole, but prior to the discrete ilmenite, calcite, chlorite and titanite. The crystals of perovskite are brown in plane-polarized light, strongly anisotropic and polysynthetically twinned. In BSE, the crystals display oscillatory-type, regular zonation (Figs. 1a, c). The individual zones are subparallel, and range in thickness from 3 to 50 μm. Their composition is similar throughout the crystal; the difference in brightness is created by varying Th (Table 3, anals. 2, 3). The primary perovskite from CAPR is compositionally similar to that occurring in phoscorites, and differs from perovskite from calcite carbonatites in containing lower Na, Nb and Fe^{3+} (Chakhmouradian & Mitchell 1997).

(iii) Overgrowths are found on early perovskite (both xenocrystic and primary). These are developed as discontinuous mantles, which intersect the primary zonation of perovskite crystals (Fig. 1a), and as linings in fractures and cavities filled with titanite, ilmenite and calcite. The thickness of the mantles ranges from a few tens of μm to 2–3 mm. In BSE, this perovskite shows much higher average atomic number (*Z*), compared to the early perovskite. The higher *Z* results from significantly higher levels of *LREE*, and lower levels of Ca and Ti (Table 3, anal. 4). To maintain charge balance, the replacement of Ca^{2+} by $LREE^{3+}$ is accompanied by incorporation of Na^{1+} in the perovskite. This compositional trend culminates with the appearance of loparite-(Ce), ideally $NaCeTi_2O_6$, in the outermost zones of the overgrowths (Table 3, anal. 5, Fig. 3a). In contrast to the primary perovskite, loparite and *LREE*-enriched perovskite show a brownish red color and weaker anisotropism in thin section.

Some loparite compositions are significantly enriched in Nb and Th (Table 3, anals. 6–9). Recalculation of these compositions into perovskite-type end-members, following the methods suggested by Mitchell (1996) and Mitchell & Chakhmouradian (1998a), indicates the existence of solid solutions toward $ThTi_2O_6$ and $NaNbO_3$ (Fig. 3). As demonstrated by the mineralogical and experimental data of Mitchell & Chakhmouradian (1999), the solid solution toward the Th-bearing end-member is limited to nearly 20–25 mol.% $ThTi_2O_6$ in loparite. The only other known occurrence of Th-rich loparite (> 20 mol.% $ThTi_2O_6$) is the Khibina complex, Kola Peninsula (Fig. 3b). Compared to Th-rich loparite from Afrikanda, that from peralkaline pegmatites of Khibina is poorer in Ca (< 1.9 wt.% CaO) and somewhat richer in Sr (up to 1.2 wt.% SrO) (Mitchell & Chakhmouradian 1998a). The enrichment of loparite from CAPR in $NaNbO_3$ delineates the lueshite evolutionary trend. This trend is characteristic for perovskite-group minerals from alkaline ultramafic and nepheline syenite complexes (Mitchell & Chakhmouradian 1996, Chakhmouradian & Mitchell 1997). After recalculation to the end-member compositions, the proportion of $NaNbO_3$ in some cases is higher than that of other end-members, and this phase should be considered to be lueshite (Fig. 3a, marked with an arrow). However, structural formulae corresponding to these compositions show the prevalence of Ti over Nb in the *B* site.

Bona fide lueshite is very rare in CAPR, and occurs solely as minute inclusions in discrete ilmenite. Lueshite from Afrikanda approaches the ideal formula $NaNbO_3$, and contains relatively low levels of Ca, Sr and Ti (Table 3, anal. 10). A characteristic feature of this mineral is high Ta (1.2–2.0 wt.% Ta_2O_5). Similarly high Ta is found in lueshite from calcite carbonatite of the Sallanlatvi complex (Kola Peninsula), but is not typical for lueshite from late dolomite carbonatites (Chakhmouradian & Mitchell 1997, 1998b). In common with lueshite from other carbonatite occurrences, that from CAPR shows significant deficiency of cations at the *A* site, ranging from 0.10 to 0.12 anions per formula unit (*apfu*).

Baddeleyite occurs in fractures within garnet and early magnetite, mostly as elongate prismatic crystals up to 30 μm in length. In CAPR, baddeleyite is the earliest Zr mineral; it was formed prior to calzirtite, zirconolite, discrete ilmenite, Zr-bearing silicates and calcite. Compositionally, baddeleyite from Afrikanda is somewhat enriched in Ti and Nb (Table 4, anals. 1–2).

Baddeleyite is a common accessory mineral in alkaline ultramafic complexes of the Kola Peninsula. This mineral is particularly ubiquitous in phoscorites and carbonatites (Rimskaya-Korsakova & Dinaburg 1964, Lapin 1979, Bulakh & Ivanikov 1984). In addition to carbonatites, baddeleyite has been described from a broad variety of silica-undersaturated rocks, including cumulates in mafic–ultramafic intrusions (Lorand & Cottin 1987, Barkov *et al.* 1995, Cabella *et al.* 1997), kimberlites (Raber & Haggerty 1979, Scatena-Wachel & Jones 1984), and carbonate parageneses of metamorphic or hydrothermal origin (Purtscheller & Tessadri 1985, Kerrich & King 1993). In common with Afrikanda (Fig. 4a), baddeleyite from carbonatite occurrences is enriched in Nb (up to 2.5 wt.% Nb_2O_5 in the Kovdor phoscorite: Kopylova *et al.* 1980, Williams 1996). However, baddeleyite in carbonatite is normally depleted in Ti. High Ti, comparable to that found in the samples from CAPR, is characteristic of baddeleyite from ultramafic cumulates (Fig. 4b and references therein). Both types of baddeleyite are virtually indistinguishable in terms of their Hf contents (Fig. 4c).

Calzirtite occurs as euhedral rectangular crystals ranging from 10 to 40 μm in size. The crystals are usually confined to fractures within garnet and early magnetite. Some crystals enclose minute fragments of relict baddeleyite. Calzirtite from CAPR shows very weak inter- and intragranular compositional variation, and

TABLE 4. REPRESENTATIVE COMPOSITIONS OF BADDELEYITE AND CALZIRTITE FROM CALCITE-AMPHIBOLE-DIOPSIDE ROCK

Wt.%	1	2	3	4
CaO	0.24	0.39	11.52	11.06
ZrO_2	97.10	93.84	67.82	67.04
TiO_2	0.42	2.08	17.94	17.45
HfO_2	1.11	1.55	n.a	n.a
Fe_2O_3	n.d	n.d	0.96	2.41
Nb_2O_5	1.04	2.33	1.31	2.15
Total	99.91	100.19	99.55	100.11
Structural formulae calculated on the basis of:	ΣO = 2		ΣO = 16	
Ca	0.005	0.008	1.828	1.745
Zr	0.972	0.928	4.898	4.815
Ti	0.006	0.032	1.998	1.933
Hf	0.006	0.009	-	-
Fe	-	-	0.107	0.267
Nb	0.010	0.021	0.088	0.143

Compositions: 1& 2 prismatic crystals of baddeleyite, 3 & 4 euhedral crystals of calzirtite. n.d = not detected; n.a = not analyzed. Total Fe is given as Fe_2O_3.

approaches the ideal formula $Ca_2Zr_5Ti_2O_{16}$ (Table 4, anals. 3–4). Calzirtite is a rare, but characteristic accessory constituent of carbonatites (Bulakh & Shevaleevskii 1962, Bulakh *et al.* 1967, 1998, Williams & Kogarko 1996). Less commonly, this mineral occurs in peridotites and kimberlites (Mitchell 1995, this work). In contrast to calzirtite from CAPR and ultramafic rocks, that from carbonatites is typically poorer in Ti (Figs. 5 a, b) and richer in Nb (Fig. 5b).

Zirconolite. In CAPR, a mineral with the general formula $CaZrTi_2O_7$ was first described under the name zirconolite (Borodin *et al.* 1956). Subsequently, $CaZrTi_2O_7$-type phases from Afrikanda and other localities at the Kola Peninsula were studied by Bulakh *et al.* (1960). These minerals form octahedral crystals, and may or may not be metamict; both non-metamict and heated metamict samples produce X-ray-diffraction patterns corresponding to the cubic fluorite-type structure (Bulakh *et al.* 1960). On the basis of these data, it has been suggested that the $CaZrTi_2O_7$-type phases from the Kola occurrences are equivalent to zirkelite (Bulakh *et al.* 1960, Kukharenko *et al.* 1965). Subsequently, the crystal structure of the type zirkelite from Jacupiranga (Brazil) has been refined as monoclinic by Pudovkina *et al.* (1974). Monoclinic symmetry has also been established for most synthetic $CaZrTi_2O_7$-type oxides, including Al, Mn, Mg, *REE*, Nb, and some actinide-doped varieties (Gatehouse *et al.* 1981, White 1984). Finally, the name zirkelite has been applied to a trigonal mineral from Campi Flegrei, Italy (Mazzi & Munno 1983). White (1984) has shown that zirconolite, zirkelite, orthorhombic polymignite and cubic pyrochlore-type structures can be regarded as polytypes derived from the fluorite structure-type. On the basis of this concept, Bayliss *et al.* (1989) have suggested a new scheme of nomenclature for the $CaZrTi_2O_7$ minerals, which has been approved by the CNMMN IMA. According to this nomenclature, the $CaZrTi_2O_7$-type phase described in the present study is classified simply as zirconolite, as its polytype has not been determined.

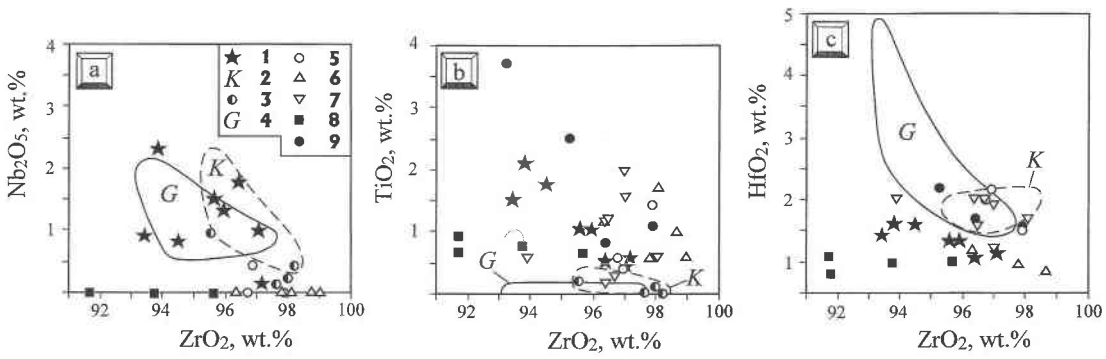

FIG. 4. Major-element variation (wt.%) in baddeleyite from calcite – amphibole – clinopyroxene rock and other occurrences. 1 Afrikanda, 2–4 carbonatites and phoscorites: 2 Kovdor, Kola (Williams 1996), 3 Sebljavr, Kola (Lapin 1979, Subbotin *et al.* 1985), 4 Guli, Siberia (Williams & Kogarko 1996), 5–8 ultramafic–mafic cumulate rocks: 5 northwestern Canada (Heaman & LeCheminant 1993), 6 Laouni, Algeria (Lorand & Cottin 1987), 7 Lukkulaisvaara and Imandrovsky, northwestern Russia (Barkov *et al.* 1995), 8 Bracco, Italy (Cabella *et al.* 1997), 9 kimberlites (South Africa) and alnöite (Île Bizard, Quebec) (Raber & Haggerty 1979, Scatena-Wachel & Jones 1984, Heaman & LeCheminant 1993).

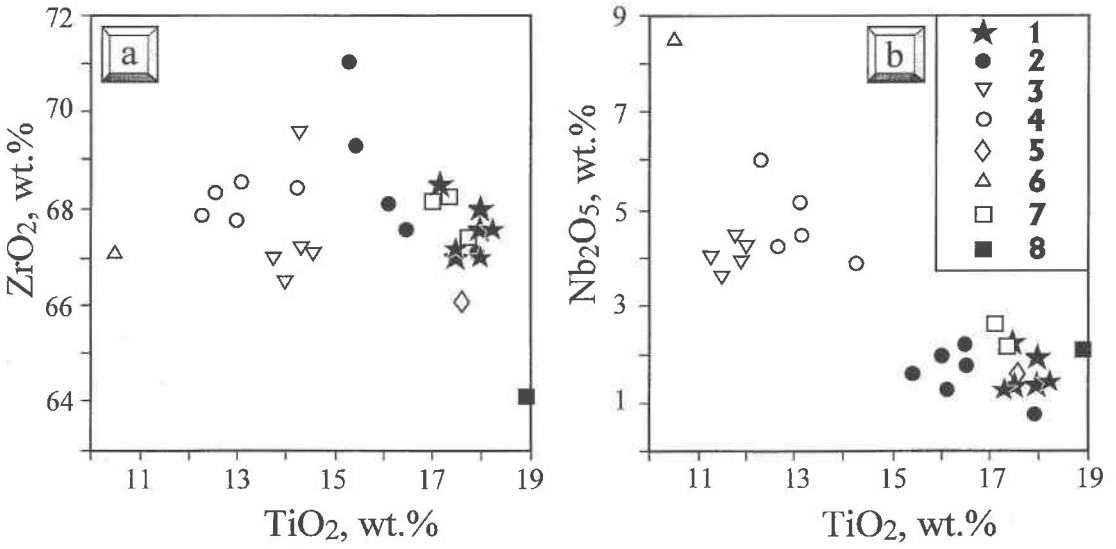

FIG. 5. Major-element variation (wt.%) in calzirtite from calcite – amphibole – clinopyroxene rock and other occurrences. 1 Afrikanda, 2–6 carbonatites and phoscorites: 2 Sebljavr, Kola (Bulakh & Shevaleevskii 1962, Lapin 1979, Subbotin *et al.* 1985), 3 Vuorijarvi, Kola (this work), 4 Guli, Siberia (Williams & Kogarko 1996), 5 Kugda, Siberia (Bulakh *et al.* 1967), 6 Kaiserstuhl, Germany (Sinclair *et al.* 1986), 7 peridotite, Khibina, Kola (this work), 8 kimberlite, Benfontein, South Africa (Mitchell 1995).

In CAPR, zirconolite occurs as euhedral to subhedral crystals up to a few millimeters across (Bulakh *et al.* 1960). The largest crystal observed in our collection is 90 μm in size. The crystals have a trigonal or hexagonal shape, and occur in fractures within garnet and magnetite. Also, zirconolite is found as an overgrowth on early magnetite and less commonly, perovskite (Fig. 6). Typically, the crystals of zirconolite are weakly zoned (Table 5, anals. 1–2). Some crystals found in association with perovskite have a thin (3 to 10 μm) discontinuous rim enriched in *LREE* and depleted in Ca. The highest rare-earth element (*REE*) content determined in the present study by energy-dispersion spectrometry is 16.3 wt.% REE_2O_3 (Fig. 7a). A re-examination of our samples by wavelength- dispersion spectrometry (WDS) gave very similar results in terms of the major and minor components, and the maximum *REE* content of 14.6 wt.% REE_2O_3 (Table 5, anal. 3). The data acquired by wavelength-dispersion spectrometry (WDS) also show that in some *REE*-rich zirconolite, Y, and not Ce, is a major element among the lanthanides (Table 5, anal. 4).

Zirconolite and other polytypes of $CaZrTi_2O_7$ occur in a variety of rocks, typically those associated with mafic, ultramafic and alkaline magmatism, as well as contact metamorphism. A comprehensive review of zirconolite occurrences worldwide has been given by Williams & Gieré (1996). A comparison of our analytical data with those available in the literature (Subbotin *et al.* 1985, Williams & Gieré 1996, Bulakh *et al.* 1998) shows that zirconolite with high *REE* contents (> 8 wt.%

TABLE 5. REPRESENTATIVE COMPOSITIONS OF ZIRCONOLITE FROM CALCITE-AMPHIBOLE-DIOPSIDE ROCK

	1	2	3	4		1	2	3	4
Wt.%					Structural formulae calculated on the basis of ΣO = 7				
CaO	12.25	11.19	8.05	8.97	Ca	0.784	0.735	0.570	0.600
MgO	0.01	n.d	0.81*	0.07	Mg	0.001	-	-	0.007
MnO	0.05	0.07	0.34	0.14	Mn	0.003	0.004	0.019	0.007
PbO	0.15	0.09	n.d	0.27	Pb	0.002	0.001	-	0.005
Y_2O_3	1.71	1.94	1.03	5.50	Y	0.054	0.063	0.036	0.183
La_2O_3	0.34	0.34	1.13	0.35	La	0.007	0.008	0.028	0.008
Ce_2O_3	2.32	2.83	7.62	2.27	Ce	0.051	0.064	0.184	0.052
Pr_2O_3	0.29	0.49	0.80	0.24	Pr	0.006	0.011	0.019	0.005
Nd_2O_3	1.09	1.44	2.68	1.21	Nd	0.023	0.032	0.063	0.027
Sm_2O_3	0.35	0.41	0.54	0.59	Sm	0.007	0.009	0.012	0.013
Gd_2O_3	0.35	0.46	0.36	0.88	Gd	0.007	0.009	0.008	0.018
Dy_2O_3	0.37	0.52	0.33	1.15	Dy	0.007	0.010	0.007	0.023
Er_2O_3	0.25	0.32	0.14	0.65	Er	0.005	0.006	0.003	0.013
ThO_2	0.21	0.53	0.22	0.03	Th	0.003	0.007	0.003	-
UO_2	0.06	0.16	n.d	0.10	U	0.001	0.002	-	0.001
SiO_2	0.23	0.24	1.88*	0.44	Si	0.014	0.015	-	0.027
ZrO_2	36.55	34.88	31.72	33.95	Zr	1.065	1.043	1.023	1.034
TiO_2	36.40	34.46	31.70	33.07	Ti	1.635	1.589	1.576	1.553
HfO_2	0.23	0.15	0.22	0.06	Hf	0.004	0.003	0.004	0.001
Al_2O_3	0.09	0.09	0.66*	0.18	Al	0.006	0.007	-	0.013
Fe_2O_3	6.86	7.38	7.76	8.38	Fe	0.308	0.341	0.386	0.394
Nb_2O_5	0.64	1.42	1.00	0.30	Nb	0.017	0.039	0.030	0.008
Ta_2O_5	0.01	0.13	0.08	0.10	Ta	-	0.002	0.001	0.002
Total	100.81	99.54	99.07	98.90					

Compositions: 1& 2 core and rim of a zoned zirconolite crystal, 3 *LREE*-rich zirconolite, 4 Y-rich zirconolite. * High concentrations of these components result from excitation of a silicate phase (? chlorite) bordering zirconolite crystal; consequently, Mg, Al and Si were not included in the structural formula for this sample. n.d = not detected. Total Fe is given as Fe_2O_3. Compositions were obtained by wavelength-dispersion spectrometry using a Cameca SX-50 electron microprobe. Operating conditions: 20 kV, 25 nA; standards for the major elements: perovskite (Ca, Ti), ZrO_2 (Zr), $NaNbO_3$ (Nb), and *REE*-silicate glasses (*REE*).

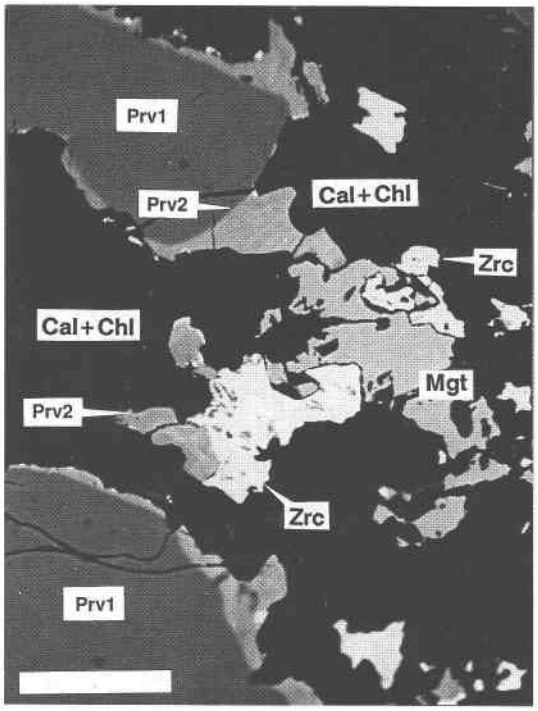

FIG. 6. Overgrowths of zirconolite (Zrc) on early magnetite (Mgt) and perovskite (Prv1, Prv2) in calcite – amphibole – clinopyroxene rock. Cal+Chl: calcite–chlorite aggregate. BSE image, scale bar is 50 μm.

REE$_2$O$_3$) is rare, but has been described in petrographically diverse environments, including carbonatites, nepheline syenites, gabbro pegmatite, sapphirine granulite and a metasomatic phlogopite rock (Fig. 7). With the exception of carbonatite, all these occurrences host zirconolite enriched in Y relative to the light *REE*. Zirconolite from carbonatite complexes invariably shows a strong predominance of Ce and Nd over Y (Williams & Gieré 1996). This pattern reflects a general geochemical feature of ultramafic alkaline rocks and associated carbonatites: a strong enrichment in *LREE* relative to the heavy rare-earth elements (*HREE*). For example, the most *REE*-rich zirconolite from the Schryburt Lake complex contains up to 19.7 wt.% *LREE*$_2$O$_3$ and only 0.4–1.5 wt.% Y$_2$O$_3$. Thus, zirconolite from Afrikanda differs from its counterparts in typical carbonatites in being generally enriched in Y (1.0–5.5 wt.% Y$_2$O$_3$), and in that both *LREE*- and Y-enriched varieties of this mineral are found in the same paragenesis.

As illustrated in Figure 7, zirconolite from Afrikanda is characterized by very low Nb [<1.6 wt.% Nb$_2$O$_5$; Borodin *et al.* (1956) reported up to 3.3 wt.% Nb$_2$O$_5$]. Zirconolite with similar Nb occurs in primitive, relatively unevolved assemblages such as contact metamorphic, and basic igneous rocks (Fig. 7, and references therein). Somewhat higher Nb (up to 9.6 wt.% Nb$_2$O$_5$) is observed in zirconolite from nepheline syenites (Platt *et al.* 1987). Finally, the highest Nb contents have been observed in zirconolite from some carbonatites (up to 24.8 wt.% Nb$_2$O$_5$: Borodin *et al.* 1961) and a mantle-derived ultrapotassic rock from Mt. Melbourne, Antarctica (up to 26.2 wt.% Nb$_2$O$_5$: Hornig & Wörner 1991).

Pyrochlore-group minerals

Pyrochlore-group minerals occur in CAPR as anhedral grains and euhedral crystals. The former type ranges from 50 to 200 μm in size, and is confined to fractures in perovskite, filled with calcite, titanite and chlorite. Other associated minerals are ilmenite, cerite-(Ce), ancylite-(Ce) and thorianite. The anhedral crystals are lemon-yellow in thin section, isotropic, and normally have a transparent clear core and a turbid fractured rim ranging from 10 to 50 μm in thickness.

Compositionally, this mineral is rich in U, Th, and Ti, and depleted in Ca and Na (Table 6, anals. 1–4). On

TABLE 6. REPRESENTATIVE COMPOSITIONS OF PYROCHLORE-GROUP MINERALS FROM CALCITE-AMPHIBOLE-DIOPSIDE ROCK

Wt.%	1*	2*	3*	4*	5*	6	7
CaO	4.09	2.13	7.72	7.65	5.83	13.69	13.36
SrO	1.08	0.95	n.d	n.d	1.17	0.78	0.58
Na_2O	n.d	n.d	n.d	n.d	0.38	7.39	7.63
La_2O_3	n.d	n.d	0.14	0.66	n.d	0.19	0.05
Ce_2O_3	4.31	4.23	4.63	4.93	2.51	0.68	0.56
Pr_2O_3	0.18	0.16	1.29	1.25	n.d	n.d	n.d
Nd_2O_3	1.79	1.28	2.57	2.48	0.97	0.10	0.11
ThO_2	10.07	4.31	28.61	29.62	14.80	n.d	n.d
UO_2	15.67	20.93	n.d	n.d	6.39	0.19	0.22
SiO_2	1.20	2.13	2.52	2.98	2.99	n.d	n.d
TiO_2	15.22	15.32	16.23	16.09	10.21	1.19	1.30
Fe_2O_3	0.49	0.34	3.19	2.89	1.83	0.49	0.48
Nb_2O_5	36.47	35.11	30.37	29.15	42.74	70.40	69.10
Ta_2O_5	1.48	1.91	n.d	n.d	0.97	2.74	2.70
Total	91.55	90.70	97.27	97.70	89.82	97.84	96.09
Structural formulae calculated on the basis of 2 B-cations:							
Ca	0.305	0.342	0.584	0.597	0.924	0.867	0.859
Sr	0.044	0.039	-	-	0.039	0.027	0.020
Na	-	-	-	-	0.002	0.847	0.888
La	-	-	0.004	0.018	0.008	0.004	0.001
Ce	0.110	0.110	0.120	0.132	0.062	0.015	0.012
Pr	0.004	0.004	0.033	0.033	-	-	-
Nd	0.032	0.020	0.065	0.064	0.016	0.002	0.002
Th	0.160	0.070	0.460	0.491	0.246	-	-
U	0.243	0.330	-	-	0.016	0.002	0.003
Ti	0.797	0.818	0.862	0.882	0.490	0.053	0.058
Fe	0.026	0.018	0.169	0.158	0.120	0.022	0.022
Nb	1.149	1.127	0.969	0.960	1.358	1.881	1.876
Ta	0.028	0.037	-	-	0.032	0.044	0.044

Compositions: 1 & 2 betafite (anhedral grain in perovskite), 3 & 4 thorium betafite (anhedral grain in perovskite), 5 thorian pyrochlore (euhedral crystal in chlorite), 6 & 7 Na-Ca pyrochlore (euhedral crystal in titanite). n.d = not detected. Total Fe is given as Fe_2O_3. * Si is not included in the structural formulae.

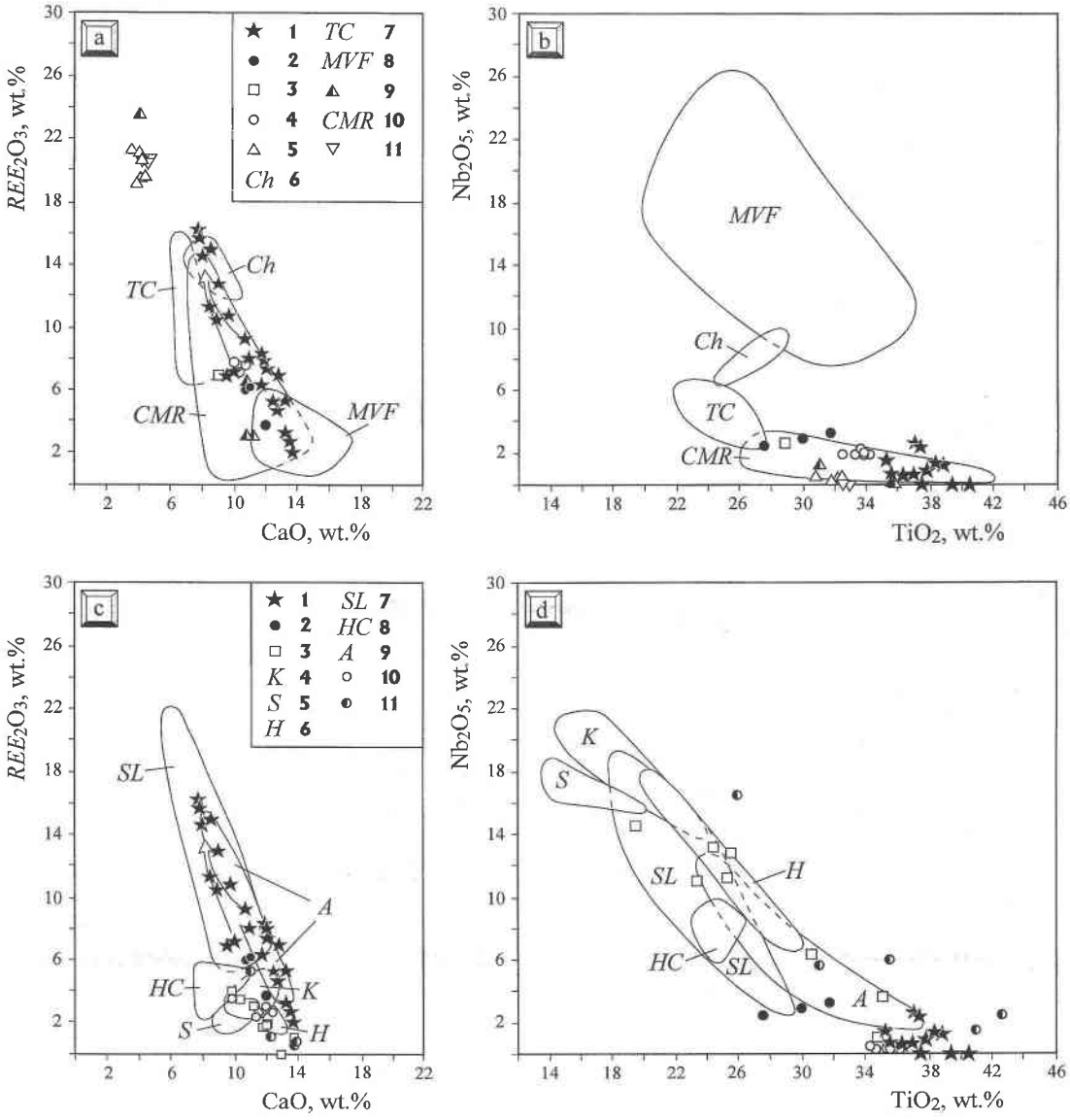

FIG. 7. Variation of REE_2O_3 *versus* CaO and Nb_2O_5 *versus* TiO_2 (wt.%) in zirconolite from calcite – amphibole – clinopyroxene rock and other occurrences. Arrow indicates evolutionary trend of zirconolite from Afrikanda. (a,b) 1–2 Afrikanda: 1 this work, 2 Borodin *et al.* (1956), Bulakh *et al.* (1960), 3 syenite, Glen Dessarry, Scotland, 4–7 nepheline syenites: 4 Pine Canyon, Utah, 5 Tchivira, Angola, 6 Chilwa, Malawi, 7 Tre Croci, Italy, 8 ultrapotassic vein in a mantle-derived xenolith, Mt. Melbourne Volcanic Field, Antarctica, 9 ultramafic and mafic cumulate rocks, 10 contact metamorphic rocks, 11 sapphirine granulite, Antarctica. (c,d) 1–2 Afrikanda: 1 this work, 2 Borodin *et al.* (1956), Bulakh *et al.* (1960), 3–10 carbonatites and phoscorites: 3 Sebljavr, Kola, 4 Kovdor, Kola, 5 Sokli, Finland, 6 Hegau, Germany, 7 Schryburt Lake, Ontario, 8 Howard Creek, British Columbia, 9 Araxá, Brazil, 10 Phalaborwa, South Africa, 11 metacarbonate rocks of alleged carbonatitic affinity, Oetztal–Stubai, Austria. Data for zirconolite from Afrikanda are from this work, unless otherwise indicated; data for zirconolite from other occurrences are from Williams & Gieré (1996), Subbotin *et al.* (1985) and Bulakh *et al.* (1998).

the basis of the nomenclature of the pyrochlore group (Hogarth 1989), this phase should be classified as betafite or "thoriobetafite", depending on whether U or Th constitutes more than 20% of a total number of *A*-site cations. However, given that "thoriobetafite" is not a valid mineral name, in this work we refer to both varieties as betafite. It is noteworthy that there is no evidence for secondary leaching of Na or Ca from this mineral; therefore, the deficiency in these elements should be considered primary.

The second morphological type consists of octahedral or, less commonly, skeletal crystals. These do not exceed a few tens of μm in size, and occur mostly in the calcite-rich zones of CAPR. This morphological type shows a wide compositional variation from thorian pyrochlore (Nb > Ti, Ta; Th ≈ 15–19% Σ*A*-cations) to nearly stoichiometric pyrochlore *sensu stricto* (Table 6, anals. 5 and 6–7, respectively).

Pyrochlore-group minerals are characteristic accessory constituents of carbonatites, phoscorites, and related metasomatic rocks. These minerals exhibit a wide compositional range with respect to *A*- and *B*-site cation substitutions, both among different petrographic units within individual carbonatite complexes and among different carbonatite complexes and provinces (Kapustin 1980, Hogarth 1989). This compositional diversity, combined with a large number of potential cationic substitutions in the pyrochlore-type structure, complicate determination of actual evolutionary trends of the pyrochlore-group minerals in carbonatites and related rocks. The compositional variation of the pyrochlore-group minerals from Afrikanda, as well as the most recent data on pyrochlore and betafite from carbonatite complexes worldwide, are shown on Figure 8 (see references therein). The early generations of pyrochlore-group minerals are typically enriched in U, Th, Ta and Ti, and occur mostly in early calcite carbonatites, phoscorites and associated fenites (Kapustin 1980, Knudsen 1989, Epshtein *et al.* 1991, Lebedeva & Nedosekova 1993, Williams 1996). Depending on the proportion of the major *B*-site cations (Nb, Ti, Ta), these minerals are represented by either uranpyrochlore (uranoan pyrochlore if U < 20% Σ*A*-cations) or betafite. The late generation of pyrochlore occurs as a rim on the early actinide-rich phase, or discrete crystals in relatively evolved calcite–dolomite, dolomite and ankerite carbonatites. This pyrochlore typically approaches the ideal formula $NaCaNb_2O_6$ (F,OH) (Kapustin 1980, Chakhmouradian & Mitchell 1998b). Rarely, pyrochlore from fresh carbonatites may contain high concentrations of *LREE*, Sr or Ba, reflecting the enrichment of late-stage carbothermal fluids in these elements (Epshtein *et al.* 1991, Chakhmouradian 1996). Primary or secondary enrichment of the pyrochlore-group minerals in *LREE*, Sr and Ba has not been observed in CAPR, and is not discussed here in detail. The mechanisms and consequences of this process are described elsewhere (Lumpkin & Ewing 1995, 1996, Wall *et al.* 1996, Chakhmouradian & Mitchell 1998b).

The evolution of pyrochlore-group minerals in CAPR defines the betafite evolutionary trend resulting from the progressive depletion in U, Th and Ti, and enrichment in Na, Ca and Nb from the early betafite through U-bearing thorian pyrochlore to late pyrochlore *sensu stricto* (Fig. 8). In most carbonatite occurrences, the depletion in actinide elements and Ti is coupled with decreasing Ta. This evolutionary trend, termed the uranpyrochlore trend in Figure 8, is commonly observed within individual grains of pyrochlore (Knudsen 1989, Hodgson & Le Bas 1992, Lebedeva & Nedosekova 1993).

Rutile (?) occurs as a product of oxidation of the ilmenite lamellae in the early magnetite (see above), and as thin (<15 μm) laths intimately intergrown with titanite replacing the discrete ilmenite. Rutile in the ilmenite lamellae is practically pure TiO_2, but an accurate determination of its composition is difficult because of the small size of the crystals. Rutile intergrown with titanite is somewhat enriched in Nb and Fe (Table 7, anal. 1). The identification in both cases as rutile rather than anatase or brookite cannot be confirmed by optical methods; thus we assume that they correspond to the most stable TiO_2 polymorph. In fact, this assumption may be incorrect, given that a secondary TiO_2 phase replacing perovskite, ilmenite and other Ti-bearing oxides in carbonate-rich rocks is typically anatase, and not rutile (Kapustin 1964, Mitchell & Chakhmouradian 1998b).

Fersmite is very rare in CAPR; prismatic crystals of this mineral are enclosed in titanite replacing the discrete ilmenite. The crystals of fersmite range from a few μm to 20 μm in length. Fersmite from Afrikanda contains appreciable Fe, Ta and Ti (Table 7, anal. 2), indicating solid solutions toward ferrocolumbite $FeNb_2O_6$, rynersonite $CaTa_2O_6$ and kassite $CaTi_2O_4(OH)_2$. Among these, ferrocolumbite and rynersonite are isostructural with fersmite, and may form a complete solid-solution series with the latter. Significant structural differences between fersmite and kassite probably limit the extent of solid solution between these two minerals to a few mole percent.

REE–Ti oxide. An unidentified oxide of *REE* and Ti is relatively common in CAPR. This mineral occurs in an assemblage with titanite, cebollite and chlorite replacing perovskite, early magnetite and ilmenite. Note that euhedral pyrochlore and fersmite occur in a similar paragenesis (see above). The *REE*–Ti oxide forms subhedral crystals of diverse morphology (cubic, elongate, platy) up to 100 μm in length at a thickness of 10–15 μm. In BSE images, some crystals show weak intricate zonation resulting from variable Nb content.

In the composition of this mineral, *LREE* (Ce > Nd > La ≈ Pr) and Ti are major cations, accompanied by minor amounts of Fe, Nb and Ca (Table 7, anals. 3–4). In the majority of Ti–Nb oxides, a structural motif is

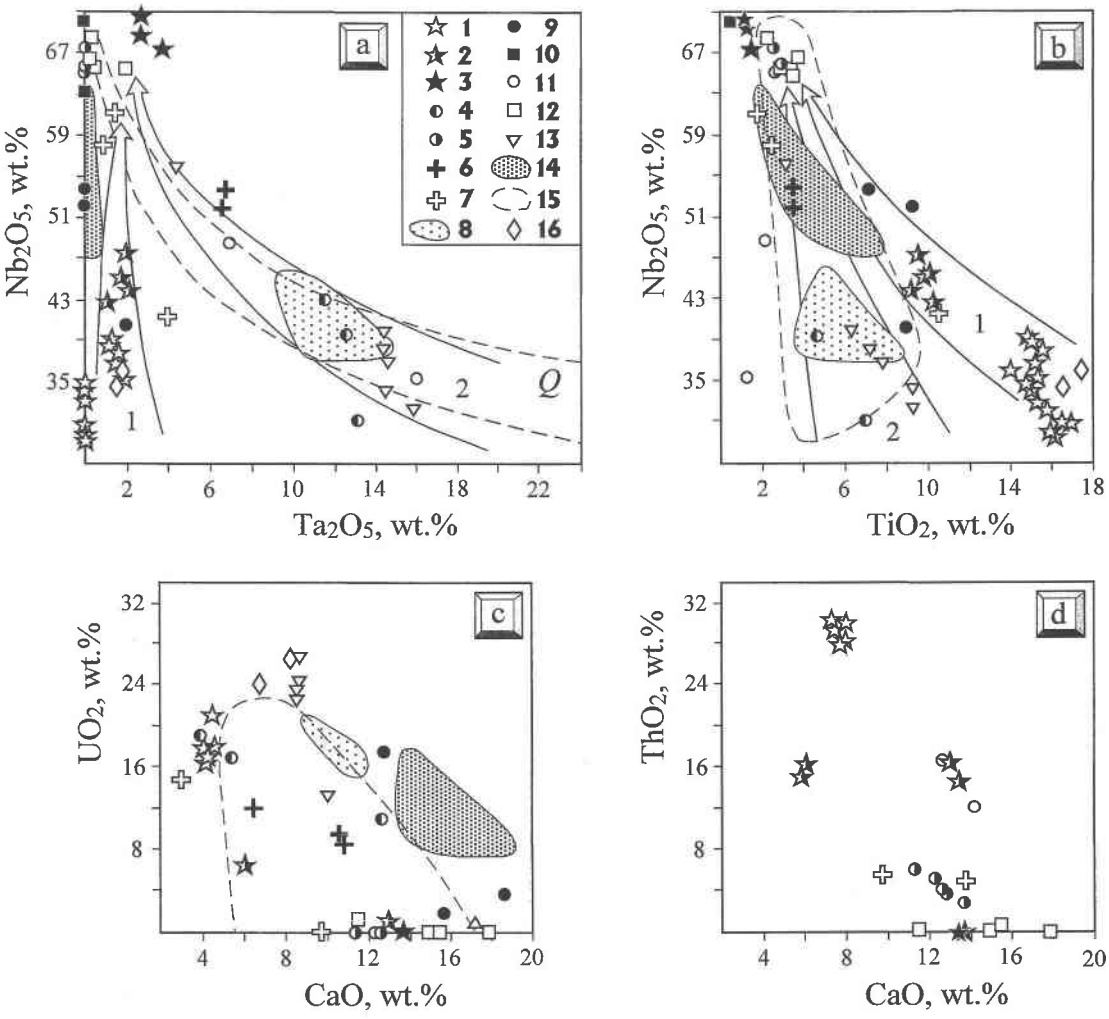

FIG. 8. Major-element variation (wt.%) in pyrochlore-group minerals from typical carbonatite occurrences and calcite – amphibole – clinopyroxene rock. Arrows indicate the betafite (1) and uranpyrochlore (2) evolutionary trends of pyrochlore-group minerals in carbonatites and related rocks. 1–3 Afrikanda: 1 betafite, 2 thorian pyrochlore, 3 pyrochlore, 4 Sebljavr, Kola (Subbotin *et al.* 1985), 5 Lesnaya Varaka, Kola (Chakhmouradian & Mitchell 1998b), 6 Sallanlatvi, Kola (this work), 7 Vuorijarvi, Kola (Epshtein *et al.* 1991), 8 Kovdor, Kola (Williams 1996), 9 Vishnevye Mts., Urals (Lebedeva & Nedosekova 1993), 10 unspecified, Siberia (Lapin & Kulikova 1989), 11 Guli, Siberia (Williams & Kogarko 1996), 12 Lueshe, Democratic Republic of Congo (Wall *et al.* 1996), 13 Fort Portal, Uganda (Hogarth & Horne 1989), 14 San Vicente, Cape Verde (Hodgson & Le Bas 1992), 15 Qaquarssuk, Greenland (Knudsen 1989). Compositions of betafite from Bancroft, Ontario (Lumpkin & Ewing 1996) are given for comparison (16).

built of six-coordinated *B*-cation (Ti, Nb, Ta, Fe^{3+}) polyhedra, whereas the number of *A*-site cations (alkaline, alkaline-earth, U, Th and *REE*) is variable. Structural formulae of these minerals are best calculated on the basis of a fixed number of *B*-site cations, two in most Ti–Nb oxides. Using this approach, we calculated an empirical formula of the *REE*–Ti oxide from Afrikanda, and found that a similar result could be obtained with recalculation on the basis of 6 oxygen atoms. Thus, stoichiometry of this mineral approaches the empirical formula $A_{1.4}B_{2.0}O_{6.0}$ (Table 7, anal. 3–4). The majority of Ti–Nb oxides have a stoichiometry close to $AB_{2.0}O_{6.0}$, and only *A*-site deficient perovskite- and pyrochlore-type phases may exhibit a cation–anion ratio similar to that observed in the Afrikanda mineral. In contrast to the *REE*–Ti oxide from CAPR, the pyrochlore-type

TABLE 7. REPRESENTATIVE COMPOSITIONS OF RUTILE, FERSMITE AND *REE*-Ti OXIDE FROM CALCITE-AMPHIBOLE-PYROXENE ROCK

Wt.%	1*	2**	3*	4*		1*	2**	3*	4*
						Structural formulae calculated on the basis of			
						ΣO = 2	Σcat = 3	ΣO = 6	
CaO	0.65	15.75	1.20	1.35	Ca	0.009	0.908	0.084	0.096
SrO	n.a	n.d	n.d	0.05	Sr	-	-	-	0.002
La_2O_3	n.a	0.06	6.08	5.99	La	-	0.001	0.147	0.146
Ce_2O_3	n.a	0.14	27.14	27.50	Ce	-	0.003	0.652	0.664
Pr_2O_3	n.a	n.d	6.53	6.75	Pr	-	-	0.156	0.162
Nd_2O_3	n.a	n.d	15.79	14.21	Nd	-	-	0.370	0.335
ThO_2	n.a	n.d	n.d	0.06	Th	-	-	-	0.001
TiO_2	94.03	4.10	34.47	32.77	Ti	0.950	0.166	1.701	1.626
FeO	n.a	2.01	n.d	n.d	Fe^{2+}	-	0.090	-	-
Fe_2O_3	2.35	n.d	4.99	4.61	Fe^{3+}	0.024	-	0.246	0.229
Nb_2O_5	3.61	73.55	1.74	4.42	Nb	0.022	1.790	0.051	0.132
Ta_2O_5	n.d	2.81	0.62	0.34	Ta	-	0.041	0.011	0.006
Total	100.64	98.42	98.56	98.05					

Compositions: 1 rutile (lamellar intergrowths with titanite replacing discrete ilmenite), 2 prismatic crystal of fersmite in titanite after ilmenite, 3 & 4 platy crystal of *REE*-Ti oxide in titanite after ilmenite. * Total Fe is given as Fe_2O_3; ** total Fe is given as FeO assuming the solid solution series fersmite $CaNb_2O_6$ - ferrocolumbite $FeNb_2O_6$. n.d = not detected; n.a = not analyzed.

phases are significantly richer in Nb plus Ta (Fig. 9 and references therein). In terms of the composition and stoichiometry, the Afrikanda material most closely matches the synthetic perovskite-type compound $Ce_{0.66}TiO_{2.9}$ (Leonov *et al.* 1966). Lucasite-(Ce) [$CeTi_2O_5(OH)$], whose composition (Nickel *et al.* 1987) also plots close to that of the Afrikanda mineral, should be ruled out on the basis of its stoichiometry. Unambiguous structural assignment of the *REE*–Ti oxide from CAPR can be done only on the basis of X-ray-diffraction studies.

Thorianite is a rare late-stage mineral in CAPR. Minute (up to 5 μm) roundish crystals of this mineral are enclosed in cerite-(Ce) and calcite filling fractures and cavities in perovskite. Thorianite from Afrikanda is nearly pure ThO_2, contains only minor Pb (~2.5 wt.% PbO) and no detectable U; however, accurate determination of its composition is impossible because of the small size of the crystals. In a very similar paragenesis (calcite, diopside, amphibole, garnet, vesuvianite, perovskite), thorianite has been found at the Turiy Mys carbonatite complex, Kola Peninsula (Bulakh & Mazalov 1974). Other occurrences of this mineral in carbonatite complexes include an apatite–phlogopite rock at Kovdor (Kola Peninsula), and carbonatites of the Kovdor (Kola), Guli (Siberia), and Phalaborwa (South Africa) intrusions (Kapustin 1964, Krasnova *et al.* 1967, Russell *et al.* 1955). Unfortunately, data on the composition of thorianite from carbonatites and related rocks are restricted to a few bulk wet-chemical

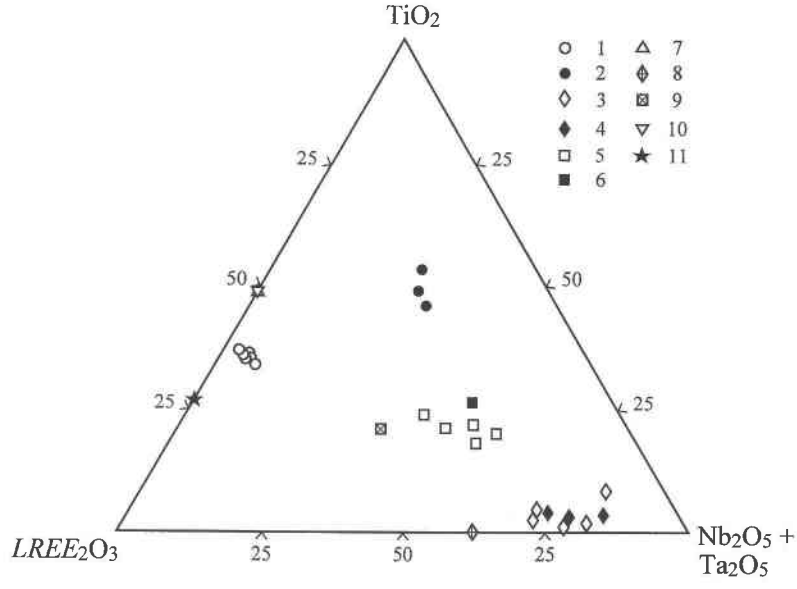

FIG. 9. Compositions of an unidentified *REE*–Ti oxide mineral from calcite – amphibole – clinopyroxene rock in comparison with other *REE*–Ti oxides. 1 Afrikanda, 2 "ceriobetafite" (Mitchell & Chakhmouradian 1998a), 3 ceriopyrochlore, Siberia (Lapin & Kulikova 1989), 4 ceriopyrochlore, Lueshe, Democratic Republic of Congo (Wall *et al.* 1996), 5 niobo-aeschynite-(Ce), Vishnevye Mountains, Urals (Lebedeva & Nedosekova 1993), 6 niobo-aeschynite-(Ce), Alaska (Rosenblum & Mosier 1975), 7 lucasite-(Ce), Argyle, Australia (Nickel *et al.* 1987), 8 ideal ceriopyrochlore $CeNb_2O_6(OH)$, 9 ideal aeschynite-(Ce) $CeTiNbO_6$, 10 $CeTi_2O_{5.6}$ (Leonov *et al.* 1966), 11 $Ce_{0.66}TiO_3$ (Leonov *et al.* 1966).

analyses. On the basis of these data, Bulakh & Mazalov (1974) suggested that the ratio Th/U in thorianite decreases from silicate-rich parageneses toward carbonatites. Our data are consistent with this observation.

Discussion and Conclusions

Genesis

Silicate–carbonate assemblages similar to the calcite – amphibole – clinopyroxene rock from the Afrikanda complex have been described in a number of alkaline ultramafic intrusions. In the Maimecha–Kotuy group of intrusions in Polar Siberia, a magnetite–diopside rock with subordinate richterite, phlogopite, calcite and apatite known as "diopsidite" is included in the phoscorite petrographic series (Egorov 1991). In contrast to typical phoscorites, clinopyroxene, and not forsterite, is the major silicate mineral in diopsidite. Hence, Egorov (1991, p. 211) proposed that this rock crystallized from phoscoritic magmas enriched in silica during their ascent. Rocks with a distinct textural and mineralogical resemblance to CAPR occur at the Turiy Mys, Kovdor and Fen carbonatite complexes (Fenno-Scandinavian Alkaline Province). A calcite – hastingsite – diopside rock from Turiy Mys contains minor perovskite and magnetite, and is believed to originate from interaction of plutonic melilitic suites with a CO_2-bearing fluid (Bulakh & Mazalov 1974, Bulakh & Ivanikov 1996). This rock is considered an early metasomatic member of the phoscorite–carbonatite petrographic series (Bulakh & Ivanikov 1996, p. 405). A similar origin has been proposed for a diopside–hastingsite rock with subordinate calcite from the Kovdor complex, Kola (Kaverin *et al.* 1988). At Fen, a calcite – hastingsite – diopside rock with minor biotite, apatite and titanite, known as "vibetoite", occurs in close spatial proximity to calcite carbonatite (Barth & Ramberg 1966). The genesis of "vibetoite" has not been discussed, but a relationship to ultramafic lamprophyre ("damkjernite") has been suggested by Barth & Ramberg (1966).

In contrast to the Kovdor and Turiy Mys complexes, melilitolites do not occur at Afrikanda; thus the crystallization of CAPR by the replacement of melilitic rocks must be ruled out. The cumulate texture comprising euhedral to subhedral clinopyroxene with interstitial opaque minerals, termed "sideronitic" in the Russian literature, is characteristic of the "diopsidite" from Maimecha–Kotuy (Egorov 1991), but is not observed in CAPR. Also lacking are brecciation, intrusive contacts, linear, flow, orbicular and spherulitic textures typical of *bona fide* magmatic phoscorites (Lapin & Vartiainen 1983, Egorov 1991). The spatially variable modal composition and, most importantly, very complex accessory mineralogy of CAPR cannot be explained in terms of simple differentiation of a parental siliceous carbonate melt.

Early thermodynamic evaluations of the system $CaO–MgO–SiO_2–H_2O–CO_2$ suggested that a volatile-rich silicate liquid precipitating diopside and other "dry" phases would not yield "low-temperature residual melts which precipitate carbonated or hydrated phases" (Wyllie 1966, p. 340). According to this author, a thermal barrier divides the vapor-saturated liquidus surface and prevents differentiation from silicate liquids to those producing carbonates; this barrier probably persists to high pressures. Subsequent studies of this quinary system have demonstrated that there are paths on the liquidus that lead from high-temperature silicate melts to those enriched in volatile components and capable of precipitating both silicate and carbonate (or hydrous) phases (Boettcher *et al.* 1980). It is also possible that addition of alkalis to the system creates alternative paths of crystallization, leading to a low-temperature carbonate melt.

Alternative models suggest formation of CAPR by replacement of the ultramafic wallrocks. A "radical" metasomatic model proposed by Kukharenko *et al.* (1965) implies interaction between the ultramafic rock-types and a juvenile CO_2-rich fluid. During this interaction, clinopyroxene and minor olivine from the wallrock were replaced by amphibole, the fluid evolved by becoming enriched in Ca, and eventually precipitated calcite (Kukharenko *et al.* 1965, p. 721). Using metasomatic rocks of the Turiy Mys complex as an example, Bulakh & Iskoz-Dolinina (1978) assessed from a thermodynamic point of view the reaction involved in the conversion of diopside to amphibole and calcite. These authors have shown that, in a reasonable range of temperatures, $P(CO_2)$ and $a(SiO_2)$, the conversion reaction occurs at moderately alkaline conditions. A "conservative" metasomatic model suggests that the parental carbonatitic melt was contaminated with silicate material derived from the ultramafic rocks. Being relatively depleted in SiO_2, this liquid precipitated magnesio-hastingsite instead of diopside, and evolved to more volatile-rich compositions. This evolution culminated with the crystallization of carbonates and hydrous phases, mostly calcite, ancylite-(Ce), chlorite and cebollite during the final stages of the formation of CAPR. In both metasomatic models, the diopside present in CAPR is assumed to be a xenocrystic phase derived from the wallrock clinopyroxenite. The diffuse contacts of CAPR with the ultramafic lithologies, silicate-rich margins and calcite-rich cores of the veins, the presence of relict perovskite and replacement textures are consistent with substantial interaction between the wallrock and the parental carbonate melt or carbothermal fluid.

The data presented in this work are, as yet, insufficient to completely discard any of the above models. A detailed examination of other mineral assemblages, in particular silicate and carbonate phases, is required to assess each of the proposed mechanisms.

Evolution of the oxide mineral assemblage

The oxide mineral assemblage in CAPR is dominated by magnetite and primary perovskite. Neither of these minerals occurs solely in carbonatites. Within ultramafic alkaline complexes, magnetite and perovskite are found in intimate association with each other, and occur virtually in all petrographic series, including ultramafic and melilitic lithologies, foidolites, carbonatites, and ultramafic lamprophyres. In silicate rocks, perovskite commonly forms a reaction rim on magnetite, not a feature observed with perovskite from carbonatites (Kukharenko *et al.* 1965, Nielsen 1980, Egorov 1991, Chakhmouradian & Mitchell 1997). This absence can be explained by the very low Ti content of magnetite in most carbonatites (see above), extraction of Ti from magnetite in the form of ilmenite prior to the formation of perovskite, or a combination of both. In CAPR, the early magnetite was relatively rich in Ti (up to 7–9 wt.% TiO_2: Kukharenko *et al.* 1965, this work). The inclusions of magnetite in the primary perovskite indicate a somewhat earlier crystallization of the former mineral. However, no reaction rim of perovskite on magnetite is observed in this rock, suggesting that the "oxyexsolution" of ilmenite from early titaniferous magnetite took place prior to the crystallization of primary perovskite. In general, the crystallization span of primary perovskite is defined by the coeval precipitation of amphibole after clinopyroxene and garnet, and by the replacement of perovskite by titanite at the contact with calcite. The Zr-oxide minerals are commonly found in fractures within the early magnetite and garnet, but not within the primary perovskite. On the other hand, calzirtite commonly encloses fragments of baddeleyite, and zirconolite occurs as an overgrowth on magnetite and, rarely, perovskite. These textural features suggest that Zr-oxide phases crystallized later than magnetite, and nearly simultaneously with perovskite, in the order from baddeleyite (ZrO_2) to calzirtite ($Ca_2Zr_5Ti_2O_{16}$), and then to zirconolite ($CaZrTi_2O_7$), reflecting a gradual increase of $a(Ca^{2+})$ in the system. It is noteworthy that the above sequence of crystallization is in agreement with those observed in carbonatites and related phoscorites from eastern Siberia and Kola Peninsula (Pozharitskaya & Samoilov 1972, Bulakh *et al.* 1998).

Further evolution of the oxide mineral assemblage can be reconstructed from the evolutionary trends exhibited by the perovskite-group minerals and zirconolite. The *LREE*-rich rim on the primary perovskite and zirconolite is discontinuous, developed locally, and intersects the primary zonation of these minerals. These morphological features rule out progressive enrichment of the *LREE* perovskite and zirconolite during growth. As discussed by Chakhmouradian & Mitchell (1997, 1998a), the enrichment in *LREE* presumably resulted from interaction of the primary oxide minerals with a CO_2-rich liquid (? fluid). Further geochemical evolution involved the enrichment of loparite ($NaCeTi_2O_6$) mantles in Nb and Th, followed by the crystallization of lueshite ($NaNbO_3$), and possibly under decreasing alkalinity, Na-depleted actinide-rich pyrochlore-group phases (betafite and thorian pyrochlore). This assemblage also includes discrete ilmenite, late magnetite and minor thorianite. These minerals crystallized earlier than titanite, chlorite and calcite, and commonly occur in fractures within the primary perovskite. Although the *LREE*, Nb, U and Th could have been partially assimilated from the dissolving perovskite, the residual liquid (? fluid) probably was a major source for these elements.

In the experimental calciocarbonatite system involving $NaLaTi_2O_6$ (Mitchell 1997), the first perovskite-type phase on the liquidus is $CaTiO_3$, whereas La is concentrated in the residuum. Eventually, this results in the formation of a reaction mantle of Ca-enriched "loparite" [(Na,La,Ca)Ti_2O_6] on the early perovskite. In experiments involving $NaNbO_3$ ($575° \leq T \leq 700°C$, $P = 1$ kbar), lueshite does not crystallize; instead, $NaNbO_3$ breaks down to form Na carbonates and Ca niobates (Mitchell 1997). Thus, the presence of $NaNbO_3$-rich compositions in CAPR indicates initially high activity of Na in the system, which is supported by the occurrence of Na-bearing carbonates in this rock (authors' unpubl. data).

The crystallization of discrete ilmenite was followed by an increase in silica activity, which shifted the equilibrium from the oxide phases toward Zr- and Ti-bearing silicate minerals. This shift is documented by the replacement of ilmenite and perovskite by titanite, baddeleyite by Zr-rich titanite and zircon, and the appearance of Ca–Zr and Th-bearing silicates in CAPR. This silicate assemblage also includes abundant chlorite, cerite-(Ce) and cebollite. In this paragenesis, oxide phases are minor and represented by *REE*–Ti oxide, fersmite, Na–Ca-bearing pyrochlore and rutile. These are intimately associated with titanite, and developed after the early Ti-bearing minerals, mostly ilmenite. Titaniferous hematite found as a thin rim on the discrete ilmenite may be either a part of this paragenesis or a product of secondary, supergene oxidation.

The relationships described above for the oxide minerals in CAPR are schematically summarized in Figure 10. All oxide phases occurring in CAPR are grouped into three major parageneses (primitive, evolved and replacement), distinguished on the basis of geochemical features, relative position in the crystallization history, and relationships with other minerals.

Conditions of formation

The compositions of coexisting magnetite and lamellar ilmenite suggest that the early stage in the formation of CAPR corresponded to a $f(O_2)$ approximately equal to 10^{-20}–10^{-22} bar (Spencer & Lindsley 1981). During crystallization of the primitive and evolved parageneses, $f(O_2)$ remained low, as documented by negligible Fe^{3+}

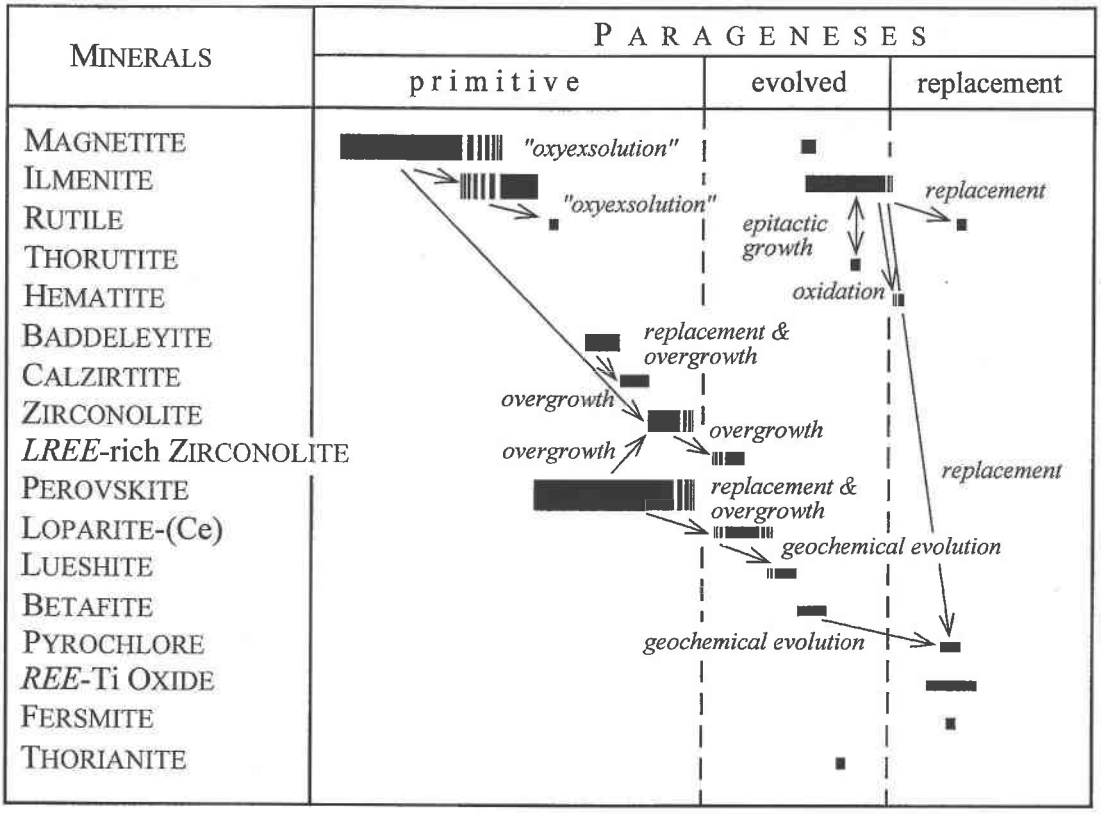

FIG. 10. Generalized paragenetic relationships of oxide minerals in the calcite – amphibole – clinopyroxene rock of the Afrikanda complex. For discussion, see text.

content in the discrete ilmenite and primary perovskite. However, some increase in $f(O_2)$ did take place late in the crystallization history, leading to the replacement of ilmenite by titaniferous hematite. Application of the ilmenite–magnetite geothermometer (Spencer & Lindsley 1981) suggests that temperatures corresponding to the separation of trellis-type lamellae from magnetite did not exceed 550°C. However, the actual temperatures could be notably in excess of 550°C, given the significant $MgTiO_3$ content (up to 23.2 mol.%) in the lamellar ilmenite from Afrikanda.

The occurrence of perovskite plus baddeleyite, but not titanite plus zircon in the primitive paragenesis, indicates very low activity of silica in the system during the early stage of crystallization. Calculations of Barker (1998) suggest the maximum $a(SiO_2)$ in the liquid approximately $10^{-1.2}$, which is significantly lower than in most alkaline silicate melts (Rass & Dubrovinskii 1997). The early precipitation of Ti-rich garnet (schorlomite) locally in the marginal zones of CAPR may indicate that $a(SiO_2)$ in the liquid increased locally owing to contamination with the silicate material from the wallrock. Alternatively, schorlomite may have precipitated at the same low $a(SiO_2)$, but under somewhat higher temperatures than perovskite, as demonstrated by thermodynamic calculations of Rass & Dubrovinskii (1997). Replacement of perovskite by titanite and precipitation of zircon in the calcite groundmass possibly resulted from an increase in $a(SiO_2)$ reflecting a decrease in temperature and transition from magmatic crystallization to formation from a fluid (D.S. Barker, pers. commun.). The lower boundary of the temperature range for the replacement paragenesis can be estimated at 400°C, as defined by the successive development of titanite and zircon. However, the possibility of contamination of the parental liquid by silicate material from the wallrock, leading to an increase in $a(SiO_2)$ and, consequently, to crystallization of titanite and zircon at somewhat higher temperatures (~500°C), should not be ruled out.

ACKNOWLEDGEMENTS

For both of us, this study may not have been possible without the constant personal encouragement from

our former scientific advisor, Prof. A.G. Bulakh. Neither may this study have been accomplished without the generous offer of Prof. R.H. Mitchell to use the instrumental facility in Lakehead University for the analytical work. We are grateful to Drs. D.S. Barker, A.G. Bulakh, R.H. Mitchell, M.J. Le Bas, R.F. Martin, N.I. Krasnova, F. Wall and C.T. Williams and an anonymous referee for numerous comments and amendments that have helped to improve the early version of the manuscript. A.J. MacKenzie is thanked for his help with the analytical work, and C.T. Williams, for obtaining the WDS analyses of zirconolite. This work was partly supported by RFBR (grant 98–05–65644) awarded to ANZ.

References

Bagdasarov, E.A. (1959): Alkaline pegmatites of the Afrikanda massif. *Zap. Vses. Mineral. Obshchest.* **88**, 261-274 (in Russ.).

_____ (1980): Microprobe study of rock-forming and ore minerals by the example of alkaline-ultrabasic massifs in Kola Peninsula. *In* Electron Probe Microanalysis in Mineralogy (Proc. 11th IMA General Meeting). Nauka Press, Leningrad, Russia (81-90; in Russ.).

Balić Žunić, T., Ščavničar, S. & Grobenski, Z. (1984): The structure of thorium (IV) dititanium (IV) oxide, $ThTi_2O_6$. *Croat. Chem. Acta* **57**, 645-651.

Barker, D.S. (1998): Silica activity in carbonatite liquids. *IAVCEI Int. Volcanol. Congress (Cape Town), Abstr. Vol.*, 6.

Barkov, A.Yu., Pakhomovskii, Ya.A. & Men'shikov, Yu.P. (1995): Baddeleyite: new occurrences from two mafic-ultramafic layered intrusions, Russia. *Mineral. Mag.* **59**, 349-353.

Barth, T.F.W. & Ramberg, I. (1966): The Fen circular complex. *In* Carbonatites (O.F. Tuttle & J. Gittins, eds.). Interscience Publishers, New York, N.Y. (225-257).

Bayliss, P., Mazzi, F., Munno, R. & White, T.J. (1989): Mineral nomenclature: zirconolite. *Mineral. Mag.* **53**, 565-569.

Boettcher, A.L., Robertson, J.K. & Wyllie, P.J. (1980): Studies in synthetic carbonatite systems: solidus relationships for CaO–MgO–CO_2–H_2O to 40 kbar and CaO–MgO–SiO_2–CO_2–H_2O to 10 kbar. *J. Geophys. Res.* **85**, 6937-6943.

Borodin, L.S., Bykova, A.V., Kapitonova, T.A. & Pyatenko, Yu.A. (1961): New data on zirconolite and its niobium variety. *Dokl. Akad. Nauk SSSR* **134**, 1022-1024 (in Russ.).

_____, Nazarenko, I.I. & Rikhter, T.L. (1956): On a new mineral zirconolite – a complex oxide of AB_3O_7 type. *Dokl. Akad. Nauk SSSR* **110**, 845-848 (in Russ.).

Bulakh, A.G., Anastasenko, G.F. & Dakhiya, L.M. (1967): Calzirtite from carbonatites of northern Siberia. *Am. Mineral.* **52**, 1880-1885.

_____, Il'inskii, G.A. & Kukharenko, A.A. (1960): Zirkelite from the deposits at the Kola Peninsula. *Zap. Vses. Mineral. Obshchest.* **89**, 261-273 (in Russ.).

_____ & Iskoz-Dolinina, I.P. (1978): Origin of carbonatites in the Central'nyy massif, Turiy peninsula. *Int. Geol. Rev.* **20**, 822-828.

_____ & Ivanikov, V.V. (1984): *The Problems of Mineralogy and Petrology of Carbonatites.* Univ. Leningrad Press, Leningrad, Russia (in Russ.).

_____ & _____ (1996): Carbonatites of the Turiy Peninsula, Kola: role of magmatism and of metasomatism. *Can. Mineral.* **34**, 403-409.

_____ & Mazalov, A.I. (1974): Accessory thorianite from the massifs of alkaline rocks and carbonatites of the Turja Peninsula (Kola Peninsula). *Am. Mineral.* **59**, 378-380.

_____, Nesterov, A.R., Anastasenko, G.F. & Anisimov, I.S. (1998a): Crystal morphology and intergrowths of calzirtite $Ca_2Zr_5Ti_2O_{16}$, zirkelite $(Ti,Ca,Zr)O_{2-x}$, zirconolite $CaZrTi_2O_7$ in phoscorites and carbonatites of the Kola Peninsula (Russia). *Neues Jahrb. Mineral., Monatsh.* (in press).

_____, _____, Williams, C.T. & Anisimov, I.S. (1998b): Zirkelite from the Sebl'yavr carbonatite complex, Kola Peninsula, Russia: an X-ray and electron microprobe study of a partially metamict mineral. *Mineral. Mag.* **62**, 837-846.

_____ & Shevaleevskii, I.D. (1962): Mineralogy and crystallography of calzirtite from alkaline rocks and carbonatites. *Zap. Vses. Mineral. Obshchest.* **91**, 14-29 (in Russ.).

Cabella, R., Gazzotti, M. & Lucchetti, G. (1997): Loveringite and baddeleyite in layers of chromian spinel from the Bracco ophiolitic unit, northern Appennines, Italy. *Can. Mineral.* **35**, 899- 908.

Chakhmouradian, A.R. (1996): On the development of niobium and rare-earth minerals in monticellite – calcite carbonatite of the Oka complex, Quebec. *Can. Mineral.* **34**, 479-484.

_____ & Mitchell, R.H. (1997): Compositional variation of perovskite-group minerals from the carbonatite complexes of the Kola alkaline province, Russia. *Can. Mineral.* **35**, 1293-1310.

_____ & _____ (1998a): Evolution of the chemical composition of perovskite from alkaline-ultramafic rocks during the metasomatism. *Zap. Vser. Mineral. Obshchest.* **127**(1), 57-68 (in Russ.).

_____ & _____ (1998b): Lueshite, pyrochlore and monazite-(Ce) from apatite–dolomite carbonatite, Lesnaya Varaka complex, Kola Peninsula, Russia. *Mineral. Mag.* **62**, 769-782.

Egorov, L.S. (1991): *Ijolite–Carbonatite Plutonism.* Nedra, Leningrad, Russia (in Russ.).

EPSHTEIN, E.M., DANIL'CHENKO, N.A. & NECHELYUSTOV, G.N. (1991): Hypogenic bariopyrochlore from a carbonatite complex. *Zap. Vses. Mineral. Obshchest.* **120**(6), 74-79 (in Russ.).

GARANIN, V.K., KUDRIAVTSEVA, G.P. & LAPIN, A.V. (1980): Typical features of ilmenite from kimberlites, alkali-ultrabasic intrusions, and carbonatites. *Int. Geol. Rev.* **22**, 1025-1050.

GASPAR, J.C. & WYLLIE, P.J. (1983a): Magnetite in the carbonatites from the Jacupiranga Complex, Brazil. *Am. Mineral.* **68**, 195-213.

_____ & _____ (1983b): Ilmenite (high Mg, Mn, Nb) in the carbonatites from the Jacupiranga complex. *Am. Mineral.* **68**, 960-971.

GATEHOUSE, B.M., GREY, I.E., HULL, R.J. & ROSSELL, H.J. (1981): Zirconolite, $CaZr_xTi_{3-x}O_7$; structure refinements for near-end-member compositions with x = 0.85 and 1.30. *Acta Crystallogr.* **B37**, 306-312.

GOTMAN, YA.D. & KHAPAEV, I.A. (1958): Thorutite – a new mineral of the group of titanates of thorium. *Zap. Vses. Mineral. Obshchest.* **87**, 201-202 (in Russ.).

GRIGOR'EV, D.P. (1965): *Ontogeny of Minerals*. Israel Program for Scientific Translations, Jerusalem, Israel.

HAGGERTY, S.E. (1991): Oxide textures – a mini-atlas. *In* Oxide Minerals: Petrologic and Magnetic Significance (D.H. Lindsley, ed.). *Rev. Mineral.* **25**, 129-220.

HEAMAN, L.M. & LECHEMINANT, A.N. (1993): Paragenesis and U–Pb systematics of baddeleyite (ZrO_2). *Chem. Geol.* **110**, 95-126.

HODGSON, N.A. & LE BAS, M.J. (1992): The geochemistry and cryptic zonation of pyrochlore from San Vicente, Cape Verde Islands. *Mineral. Mag.* **56**, 201-214.

HOGARTH, D.D. (1989): Pyrochlore, apatite and amphibole: distinctive minerals in carbonatites. *In* Carbonatites: Genesis and Evolution (K. Bell, ed.). Unwin Hyman, London, U.K. (105-148).

_____ & HORNE, J.E.T. (1989): Non-metamict uranoan pyrochlore and uranpyrochlore from tuff near Ndale, Fort Portal area, Uganda. *Mineral. Mag.* **53**, 257-262.

DE HOOG, J.C.M. & VAN BERGEN, M.J. (1997): Notes on the chemical composition of zirconolite with thorutite inclusions from Walaweduwa, Sri Lanka. *Mineral. Mag.* **61**, 721-725.

HORNIG, I. & WÖRNER, G. (1991): Zirconolite-bearing ultrapotassic veins in a mantle-xenolith from Mt. Melbourne Volcanic Field, Victoria Land, Antarctica. *Contrib. Mineral. Petrol.* **106**, 355-366.

KAPUSTIN, YU.L. (1964): Accessory rare-metal mineralogy of carbonatites at Kola Peninsula. *In* Mineralogy and Genetic Peculiarities of Alkaline Massifs. Nauka Press, Moscow, Russia (135-194; in Russ.).

_____ (1980): *Mineralogy of Carbonatites*. Amerind Publishing Co, New Delhi, India.

KAVERIN, S.V., KRASNOVA, N.I. & TARASENKO, YU.N. (1988): On the mineralogy of apomelilitic rocks of the Kovdor massif. *In* Mineralogy and Geochemistry VII. Leningrad University Press, Leningrad, Russia (46-62; in Russ.).

KERRICH, R. & KING, R. (1993): Hydrothermal zircon and baddeleyite in Val-d'Or Archean mesothermal gold deposits: characteristics, compositions, and fluid-inclusion properties, with implications for timing of primary gold mineralization. *Can. J. Earth Sci.* **30**, 2334-2351.

KNUDSEN, C. (1989): Pyrochlore group minerals from the Qaqarssuk carbonatite complex. *In* Lanthanides, Tantalum and Niobium (P. Möller, P. Černý & F. Saupé, eds.). Springer-Verlag, Berlin, Germany (80-99).

_____ (1991): Petrology, geochemistry and economic geology of the Qaquarssuk carbonatite complex, southern West Greenland. *Mineral. Deposita, Monogr.* **29**.

KOPYLOVA, L.N., KRASNOVA, N.I., MARTOVITSKAYA, N.A. & PORITSKAYA, L.G. (1980): Typochemical features of calcite and baddeleyite from the Kovdor complex deposit. *In* Alkaline Magmatism and Apatite Potential of the Siberian North. NIIGA Press, Leningrad, Russia (124-138; in Russ.).

_____, _____ & SULIMOV, B.I. (1985): On a new ore type from the Kovdor complex deposit. *In* Petrography and Minerageny of Alkaline, Alkaline-Ultramafic and Carbonatite Complexes of the Kola–Karelian Region. Kola Sci. Center Press, Apatity, Russia (69-76; in Russ.).

KRAMM, U., KOGARKO, L.N., KONONOVA, V.A. & VARTIAINEN, H. (1993): The Kola alkaline province of the CIS and Finland: precise Rb–Sr ages define 380–360 Ma range for all magmatism. *Lithos* **30**, 33-44.

KRASNOVA, N.I. & BALMASOV, E.L. (1987): On the nature of intergrowths in magnetites. *Mineral. Zh.* **9**, 53-61 (in Russ.).

_____ & KREZER, YU.L. (1995): New data on the nature of fine and ultrafine lamellae in titanomagnetite. *Eur. J. Mineral.* **7**, 1361-1372.

_____, KARTENKO, N.F., RIMSKAYA-KORSAKOVA, O.M. & FIRYULINA, V.V. (1967): Thorianite from phlogopite-bearing rocks of the Kovdor massif (Kola Peninsula). *In* Mineralogy and Geochemistry II. Leningrad University Press, Leningrad, Russia (19-27; in Russ.).

_____, NESTEROV, A.R. & KREZER, YU.L. (1991): On the composition of intergrowths in some magnetites. *Zap. Vses. Mineral. Obshchest.* **120**(6), 44-56 (in Russ.).

KUKHARENKO, A.A. & BAGDASAROV, E.A. (1961): Perovskites from ultramafic-alkaline rocks of the Kola Peninsula. *Trudy VSEGEI, new ser.* **45**(2), 37-66 (in Russ.).

_____, BULAKH, A.G., IL'INSKII, G.A., SHINKAREV, N.F. & ORLOVA, M.P. (1971): *Metallogenic Peculiarities of Alkaline Formations of the Eastern Part of the Baltic Shield.* Trudy LOE (Leningrad Natur. Soc.), Leningrad, Russia (in Russ.).

_____, ORLOVA, M.P., BULAKH, A.G., BAGDASAROV, E.A., RIMSKAYA-KORSAKOVA, O.M., NEFEDOV, E.I., IL'INSKII, G.A., SERGEEV, A.S. & ABAKUMOVA, N.B. (1965): *The Caledonian Complex of Ultrabasic Alkaline Rocks and Carbonatites of the Kola Peninsula and Northern Karelia.* Nedra Press, Leningrad, Russia (in Russ.).

KUPLETSKII, B.M. (1938): The pyroxenite intrusion near Afrikanda Station on the Kola Peninsula. *Trudy Petrograph. Inst., Akad. Nauk SSSR* **12**, 71-88 (in Russ.).

LAPIN, A.V. (1979): Mineral parageneses of apatite ores and carbonatites of the Sebl'yavr massif. *Int. Geol. Rev.* **21**, 1043-1052.

_____ & KULIKOVA, I.M. (1989): Processes of pyrochlore alteration and their products in the carbonatite weathering crusts. *Zap. Vses. Mineral. Obshchest.* **118**(1), 41-49 (in Russ.).

_____ & VARTIAINEN, H. (1983): Orbicular and spherulitic carbonatites from Sokli and Vuorijarvi. *Lithos* **16**, 53-60.

LEBEDEVA, I.O. & NEDOSEKOVA, I.L. (1993): On the process of aeschynitization of pyrochlore from carbonatites of the Buldymskii massif (Vishnevye Mts., Urals). *Zap. Vser. Mineral. Obshchest.* **122**(2), 69-75 (in Russ.).

LEONOV, A.I., PIRYUTKO, M.M. & KELER, E.K. (1966): Influence of the gas medium and temperature on the reaction in the system Ce–Ti–O and comparison of the properties of titanates of rare earth elements. *Inorg. Anal. Chem. (Bull. Akad. Nauk ΣR, Chem. Sci. Div.)* **1966**(5), 756-760.

LORAND, J.P. & COTTIN, J.Y. (1987): A new natural occurrence of zirconolite ($CaZrTi_2O_7$) and baddeleyite (ZrO_2) in basic cumulates: the Laouni layered intrusion (southern Hoggar, Algeria). *Mineral. Mag.* **51**, 671-676.

LUMPKIN, G.R. & EWING, R.C. (1995): Geochemical alteration of pyrochlore-group minerals: pyrochlore subgroup. *Am. Mineral.* **80**, 732-743.

_____ & _____ (1996): Geochemical alteration of pyrochlore-group minerals: betafite subgroup. *Am. Mineral.* **81**, 1237-1248.

MAZZI, F. & MUNNO, R. (1983): Calciobetafite (new mineral of the pyrochlore group) and related minerals from Campi Flegrei, Italy; crystal structures of polymignite and zirkelite: comparison with pyrochlore and zirconolite. *Am. Mineral.* **68**, 262-276.

MITCHELL, R.H. (1978): Manganoan magnesian ilmenite and titanian clinohumite from the Jacupiranga carbonatite, Sao Paulo, Brazil. *Am. Mineral.* **63**, 544-547.

_____ (1995): Accessory rare earth, strontium, barium and zirconium minerals in the Benfontein and Wesselton calcite kimberlites, South Africa. *In* Kimberlites, Related Rocks and Mantle Xenoliths (H.O.A. Meyer & O.H. Leonardos, eds.). Companhia Pesquisa Recursos Minerals, Rio de Janeiro, Brazil (115-128).

_____ (1996): Perovskites: a revised classification scheme for an important rare earth element host in alkaline rocks. *In* Rare Earth Minerals: Chemistry, Origin and Ore Deposits (A.P. Jones, F. Wall & C.T. Williams, eds.). *Mineral. Soc., Ser.* **7**. Chapman & Hall, London, U.K. (41-76).

_____ (1997): Preliminary studies of the solubility and stability of perovskite group compounds in the synthetic carbonatite system calcite–portlandite. *J. Afr. Earth Sci.* **25**, 147-158.

_____ & CHAKHMOURADIAN, A.R. (1996): Compositional variation of loparite from the Lovozero alkaline complex, Russia. *Can. Mineral.* **34**, 977-990.

_____ & _____ (1998a): Th-rich loparite from the Khibina alkaline complex, Kola Peninsula: isomorphism and paragenesis. *Mineral. Mag.* **62**, 341-353.

_____ & _____ (1998b): Instability of perovskite in a CO_2-rich environment: examples from carbonatite and kimberlite. *Can. Mineral.* **36**, 939-951.

_____ & _____ (1999): Solid solubility in the system $NaLREETi_2O_6 – ThTi_2O_6$ (LREE, light rare-earth elements): experimental and analytical data. *Phys. Chem. Minerals* (in press).

NICKEL, E.H., GREY, I.E. & MADSEN, I.C. (1987): Lucasite-(Ce), $CeTi_2(O,OH)_6$, a new mineral from Western Australia: its description and structure. *Am. Mineral.* **72**, 1006-1010.

NIELSEN, T.F.D. (1980): The petrology of a melilitolite, melteigite, carbonatite and syenite ring dike system, in the Gardiner complex, East Greenland. *Lithos* **13**, 181-197.

ORLOVA, M.P. (1993): Middle-Late Paleozoic riftogenic system. *In* Magmatism and Metallogeny of the Riftogenic Systems of the Eastern Baltic Shield. Nedra Press, St. Petersburg, Russia (143-160; in Russ.).

PEKOV, I.V., PETERSEN, O.V. & VOLOSHIN, A.V. (1997): Calcio-ancylite-(Ce) from Ilimaussaq and Narssarssuk, Greenland, Kola Peninsula and Polar Urals, Russia: ancylite-(Ce) – calcio-ancylite-(Ce) an isomorphous series. *Neues Jahrb. Mineral., Abh.* **171**, 309-322.

PLATT, R.G., WALL, F., WILLIAMS, C.T. & WOOLLEY, A.R. (1987): Zirconolite, chevkinite and other rare earth minerals from nepheline syenites and peralkaline granites and

syenites of the Chilwa alkaline province, Malawi. *Mineral. Mag.* **51**, 253-263.

POZHARITSKAYA, L.K. & SAMOILOV, V.S. (1972): *Petrology, Mineralogy and Geochemistry of East- Siberian Carbonatites*. Nauka Press, Moscow, Russia (in Russ.).

PRINS, P. (1972): Composition of magnetite from carbonatites. *Lithos* **5**, 227-240.

PUDOVKINA, Z.V., DUBAKINA, L.S., LEBEDEVA, S.I. & PYATENKO, YU.A. (1974): Brazilian zirkelite. *Zap. Vses. Mineral. Obshchest.* **103**, 368-372 (in Russ.).

PURTSCHELLER, F. & TESSADRI, R. (1985): Zirconolite and baddeleyite from metacarbonates of the Oetztal–Stubai complex (northern Tyrol, Austria). *Mineral. Mag.* **49**, 523-529.

RABER, E. & HAGGERTY, S.E. (1979): Zircon oxide reactions in diamond-bearing kimberlites. *In* Kimberlites, Diatremes and Diamonds: their Geology, Petrology and Geochemistry **1** (Proc. Second Int. Kimberlite Conf.; F.R. Boyd & H.O.A. Meyer, eds.), 229-240.

RASS, I.T. & DUBROVINSKII, L.S. (1997): The thermodynamic parameters and stability region of schorlomite. *Dokl. Russ. Acad. Sci., Earth Sci. Sect.* **355**, 730-732.

RIMSKAYA-KORSAKOVA, O.M. & DINABURG, I.B. (1964): Baddeleyite in the alkaline ultramafic massifs of the Kola Peninsula. *In* Mineralogy and Geochemistry **I**, Leningrad University Press, Leningrad, Russia (13-30; in Russ.).

ROSENBLUM, S. & MOSIER, E.L. (1975): Nonmetamict nioboaeschynite-(Ce) from Alaska. *Am. Mineral.* **60**, 309-315.

RUSSELL, H.D., HIEMSTRA, S.A. & GROENEVELD, D. (1955): The mineralogy and petrology of the carbonatite at Loolekop, eastern Transvaal. *Trans. Geol. Soc. S. Afr.* **58**, 197-208.

SCATENA-WACHEL, D.E. & JONES, A.P. (1984): Primary baddeleyite (ZrO_2) in kimberlite from Benfontein, South Africa. *Mineral. Mag.* **48**, 257-261.

SECHER, K. & LARSEN, L.M. (1980): Geology and mineralogy of the Sarfartôq carbonatite complex, southern West Greenland. *Lithos* **13**, 199-212.

SINCLAIR, W., EGGLETON, R.A. & MCLAUGHLIN, G.M. (1986): Structure refinement of calzirtite from Jacupiranga, Brazil. *Am. Mineral.* **71**, 815-818.

SPENCER, K.J. & LINDSLEY, D.H. (1981): A solution model for coexisting iron–titanium oxides. *Am. Mineral.* **66**, 1189-1201.

STRECKEISEN, A. (1978): Classification and nomenclature of volcanic rocks, lamprophyres, carbonatites and melilitic rocks. *Neues Jahrb. Mineral., Abh.* **134**, 1-14.

SUBBOTIN, V.V., KIRNARSKII, YU.M., KURBATOVA, G.S., STREL'NIKOVA, L.A. & SUBBOTINA, G.F. (1985): Composition of apatite-bearing rocks of the central part of the Sebl'javr massif. *In* Petrography and Minerageny [sic] of Alkaline, Alkaline-Ultramafic and Carbonatite Complexes of the Kola–Karelian Region. Kola Sci. Center Press, Apatity, Russia (61-69; in Russ.).

WALL, F., WILLIAMS, C.T. & WOOLLEY, A.R. (1996): Pyrochlore from weathered carbonatite at Lueshe, Zaire. *Mineral. Mag.* **60**, 731-750.

WHITE, T.J. (1984): The microstructure and microchemistry of synthetic zirconolite, zirkelite and related phases. *Am. Mineral.* **69**, 1156-1172.

WILLIAMS, C.T. (1996): The occurence of niobian zirconolite, pyrochlore and baddeleyite in the Kovdor carbonatite complex, Kola Peninsula, Russia. *Mineral. Mag.* **60**, 639-646.

_____ & GIERÉ, R. (1996): Zirconolite: a review of localities worldwide, and a compilation of its chemical compositions. *Bull. Nat. Hist. Museum London* **52**, 1-24.

_____ & KOGARKO, L.N. (1996): New data on rare-metal mineralization in carbonatites of the Guli massif, Polar Siberia. *Geokhimiya* **1996**(6), 483-491 (in Russ.).

WYLLIE, P.J. (1966): Experimental studies of carbonatite problems: the origin and differentiation of carbonatite magmas. *In* Carbonatites (O.F. Tuttle & J. Gittins, eds.). Interscience Publishers, New York N.Y. (311-352).

ZAITSEV, A. & BELL, K. (1995): Sr and Nd isotope data of apatite, calcite and dolomite as indicators of source, and the relationships of phoscorites and carbonatites. *Contrib. Mineral. Petrol.* **121**, 324- 335.

Received June 22, 1998, revised manuscript accepted February 26, 1999.